

NASA Contractor Report 3710

19951226 100

# Critical Joints in Large Composite Aircraft Structure

**Willard D. Nelson,  
Bruce L. Bunin, and  
Leonard John Hart-Smith**

**CONTRACT NAS1-16857**  
**AUGUST 1983**

DISTRIBUTION STATEMENT  
Approved for public release  
Distribution Unlimited

**25**

25th Anniversary  
1958-1983

NASA

## BRIC QUALITY MANAGEMENT

# NASA Contractor Report 3710

## Critical Joints in Large Composite Aircraft Structure

**Willard D. Nelson,  
Bruce L. Bunin, and  
Leonard John Hart-Smith  
*Douglas Aircraft Company*  
*McDonnell Douglas Corporation*  
*Long Beach, California***

**Prepared for  
Langley Research Center  
under Contract NAS1-16857**

Accesion For	
NTIS	CRA&I
DTIC	TAB
Unannounced	
Justification	
By _____	
Distribution / _____	
Availability Codes	
Dist	Avail and / or Special
A-1	



National Aeronautics  
and Space Administration

Scientific and Technical  
Information Branch

1983

## CRITICAL JOINTS IN LARGE COMPOSITE AIRCRAFT STRUCTURE

WILLARD D. NELSON  
Project Manager

BRUCE L. BUNIN  
Engineer-Scientist Specialist

LEONARD JOHN HART-SMITH  
Principal Engineer-Scientist

Douglas Aircraft Company  
McDonnell Douglas Corporation  
Long Beach, California 90846

### ABSTRACT

A program was conducted at Douglas Aircraft Company under NASA-Langley Contract NAS1-16857 to develop the technology for critical structural joints of composite wing structure that meets design requirements for a 1990 commercial transport aircraft. The prime objective of the program was to demonstrate the ability to reliably predict the strength of large bolted composite joints. Ancillary testing of 180 specimens generated data on strength and load-deflection characteristics which provided input to the joint analysis. Load-sharing between fasteners in multirow bolted joints was computed by the nonlinear analysis program A4EJ. This program was used to predict strengths of 20 additional large subcomponents representing strips from a wing root chordwise splice. In most cases, the predictions were accurate to within a few percent of the test results. In some cases, the observed mode of failure was different than anticipated. The highlight of the subcomponent testing was the consistent ability to achieve gross-section failure strains close to 0.005. That represents a considerable improvement over the state of the art.

### NOMENCLATURE

C	reduction factor and compliance coefficient
d	bolt or hole diameter
d/t	diameter-to-thickness ratio
d/w	diameter-to-width ratio
E	Young's modulus
EI	bending stiffness
e	edge distance

e/d	edge distance-to-diameter ratio
F	allowable stress
f	operating stress
G	shear modulus
GJ	torsional stiffness
K	elastic spring rate
k	bolt efficiency factor
$k_{tc}$	composite stress concentration factor
$k_{te}$	elastic stress concentration factor
$N_x$	load intensity
P	bolt or joint load
t	thickness
w	width
w/d	width-to-diameter ratio
$\beta$	coefficient
$\Delta$	increment
$\delta$	displacement
$\sigma$	stress
$\bar{\sigma}$	average stress

## SUBSCRIPTS

bb	bolt bending
bbr	bolt bearing
brg	bearing
bru	bearing ultimate
bry	bearing yield
bs	bolt shear
cu	compression ultimate
p	plate
pbr	plate bearing
tu	tension ultimate
ult	ultimate

## 1. INTRODUCTION

The major objective of this investigation was to develop and demonstrate the technology for critical structural joints of a composite wing structure that meets all the design requirements of a 1990 commercial transport aircraft.

To fulfill this objective, analytical procedures were developed for joint design and analysis. Specimen testing was conducted on single-bolt joints to provide empirical data for the analysis formulas to provide empirical data for the analysis formulas and to compare the analytical predictions for structurally configured joints with results of tests on multirow joints. The agreement was found to be very good and, more importantly, the use of the A4EJ computer analysis program permitted the design of

large bolted joints which usually failed at a gross section strain of about 0.005. This represents a considerable improvement over the current state of the art for highly loaded bolted joints in composite structures. The load intensities were on the order of 40,000 to 45,000 pounds per inch of specimen width for 1.0-inch-thick graphite-epoxy laminates.

The work was conducted by Douglas Aircraft Company, at Long Beach, California, under contract to NASA-Langley Research Center. Significant work on which this research was based includes an earlier NASA-Langley contract on small bolted coupon tests in which the failure mechanisms and strengths for composite laminates adjacent to bolt holes were characterized empirically (see Hart-Smith [1]). That work, in turn, was followed by a recent contract with the U.S. Air Force Flight Dynamics Laboratory at Wright-Patterson AFB, Ohio, in which one task was to develop the A4EJ nonlinear computer program for load-sharing in multirow bolted joints (see Hart-Smith [2]). Other related work will be discussed in the paper.

The analysis of load transfer through mechanically fastened joints in fibrous composite laminates must inevitably rely upon some empirically derived input based on test results. This is so because fiber-reinforced resins do not fail as homogeneous one-phase materials, although they are usually modeled as such, but as heterogeneous materials with two distinct phases and an interface. As shown in Figure 1, the efficiency of real composite bolted joints lies roughly halfway between analytical predictions based on purely elastic and perfectly plastic behavior. Analysis based on either extreme does not come close to predicting the strength of these single-row bolted joints, and either extreme would not be acceptable for design purposes without some form of major modification. All analyses of composite bolted joints rely on an empirical correlation factor in some form or other. In the case of the A4EJ analysis program, the correlation is achieved by modifying the theoretical elastic stress concentration factor at each bolt hole. The stress concentration factor is reduced, on the basis of test results, to reflect a failure mechanism which starts with fiber pull-out from the resin over a finite length in the most highly strained areas and proceeds through delaminations around the bolt holes before any fibers are broken.

Estimation of stress concentration factors by the BJSFM method (Garbo and Ogonowski [3]) allows for this apparent nonlinear behavior in the immediate vicinity of the bolt holes by comparing the laminate stresses with elastic failure criteria at a distance slightly offset from the edge of the hole. For example, an offset of 0.020 inch has been found to be effective in predicting the initiation of damage, which can be matched with the applied limit loads as a design approach. Not all methods make the correlation factor so evident, but they all employ one in some form or other to relate the theories and experiments.

The need to characterize this failure mechanism of bolted joints in composites is one of the reasons why bolted joints of various sizes were tested in this investigation. Another reason for the testing was the need to acquire load deflection, or stiffness, measurements to permit determination of the load-sharing between the various fasteners. These test results have shown that an old NACA formula for the stiffness of bolted joints in metal structures (Tate and Rosenfeld [4]) needed only a minor modification to account for the different moduli associated with orthotropic composite laminates. The formula, which is defined later, can be used with confidence to predict the elastic part of the load deflection curve. Such a curve is approximated by two straight lines in Figure 2. It appears that the precise definition of the nonlinear portion of this characteristic is not critical, provided that the bearing strength cutoff is reasonable. The explanation of this phenomenon seems to be that tension-through-the-hole failures are associated with the elastic part of the load deflection curve at one particular fastener while, if the failure

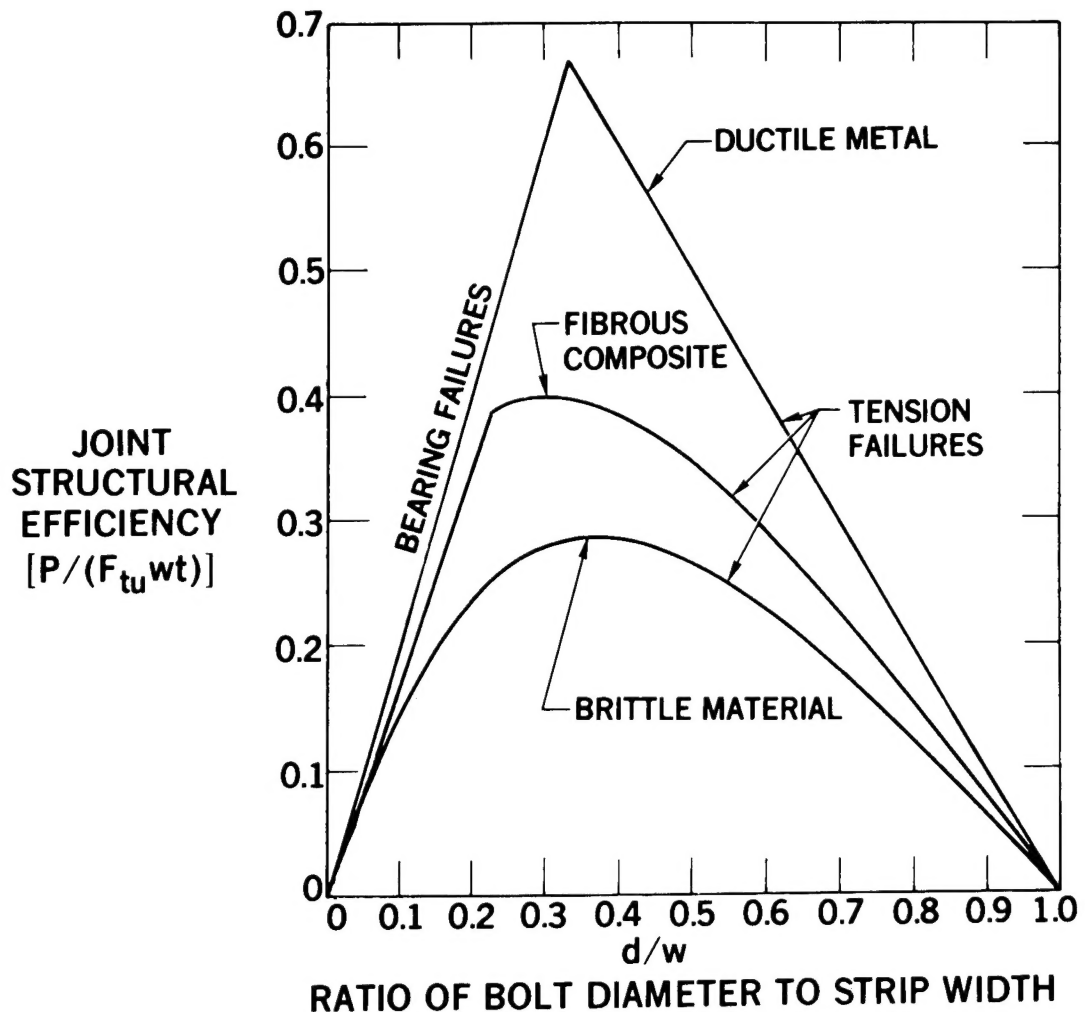


FIGURE 1. RELATION BETWEEN STRENGTHS OF BOLTED JOINTS IN DUCTILE, FIBROUS COMPOSITE AND BRITTLE MATERIALS

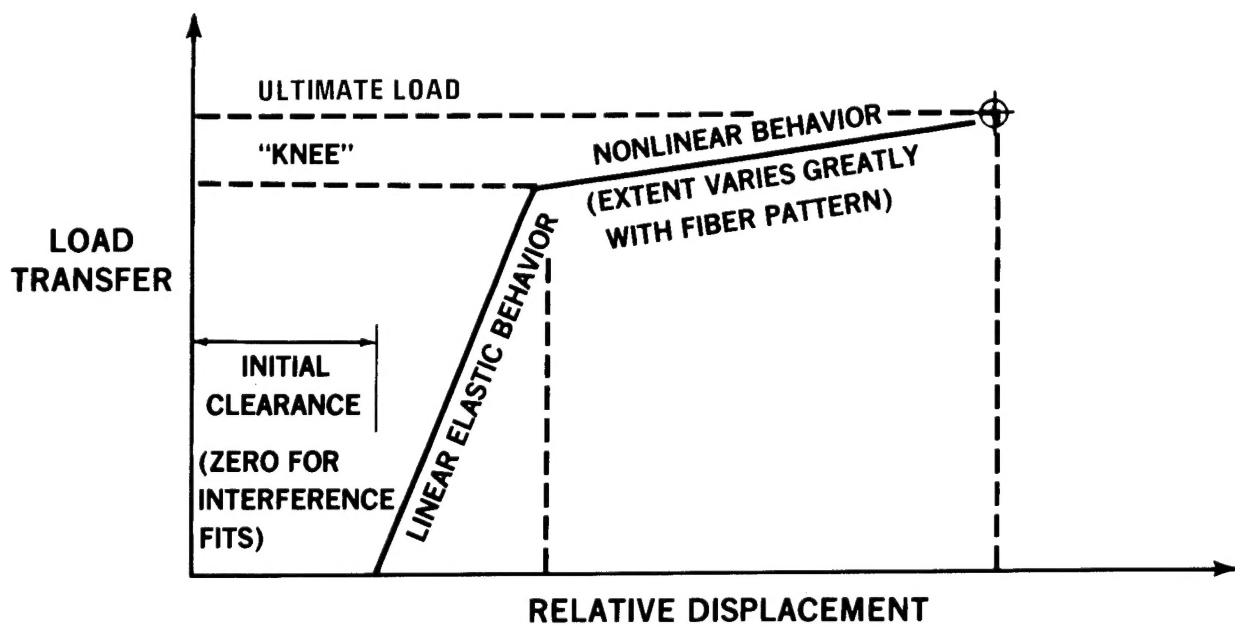


FIGURE 2. FASTENER LOAD DEFLECTION CHARACTERISTICS

mode is in bearing, the deformations at the bolt hole prior to ultimate failure are so large as to be unacceptable for design practice. Usually, all other fasteners in the joint are less critically loaded and their load deflection characteristic is important only in making the correct determination of the load-sharing between the fasteners.

The stiffness and failure data generated on single fastener joints were used successfully to predict the failure load of various structurally configured multirow bolted joints. Sample comparisons between test and theory are included below.

The relative structural efficiencies of joints of different configurations have been assessed here in order to understand the best approach to designing joints which permit the basic skin laminates to be operated at as high a strain as possible (thereby minimizing the weight of the major components). The best such solutions are associated with apparently overreinforced splice plates to minimize the bearing stress in the skin at the outermost row of fasteners, where the bypass stress is highest. However, since the bearing and tension allowables for a skin are higher than for the splice plates between which it is sandwiched, some of the reinforcement of the splices used to modify the distribution of the bolt load transfer would also be needed for strength.

In addition to testing and analysis of idealized joints, treated as strips isolated out of an entire structure, consideration has been given to the practical constraints of a complete design. These include manufacturing breaks, spar caps, and loading by torque as well as by wing-bending loads. Design layouts have been prepared for an all-composite wing, suitable for some future wide-bodied transport aircraft, to define the three-dimensional configuration of such joints.

## 2. MATERIAL AND FIBER PATTERN SELECTION

The fibrous composite material used in this program is a graphite-epoxy unidirectional tape with Toray high-strength T300 fibers and Ciba Geigy 914 resin. The ply thickness was twice the normal 0.005 inch and produced cured laminates of 0.0104 inch per ply. The considerations behind these selections are presented in the following text. The T300 generic fiber is in widespread use in industry, even though new fibers with higher strain-to-failure are becoming available now. The 914 resin was selected as the toughened resin for which the greatest data base was available and as a material of known good handling characteristics for layup.

The thickened plies were adopted to minimize the number of plies and layup operations needed for a thick wing skin and to reduce the cost of this test program. It appears in retrospect that the added toughness of the resin was counteracted by the consequent doubling of the shear load on each resin interface. The joint strengths attained do not represent a quantum improvement with respect to state-of-the-art brittle resins and thinner plies of fibers. However, the strengths were usually higher, mainly because of the larger softened zone around the bolt holes and the consequent increase in bypass strength. Also, the thickened plies impose more severe constraints than thinner plies on the minimum gage of balanced laminates. These thickened plies would not be preferred for thin-skinned secondary structure and would need justification on the basis of complete comparative designs on large, thick structure like transport aircraft skins which, themselves, become relatively thin outboard.

Two fiber patterns were selected to encompass the practical range of fiber pattern options. One was pseudoisotropic Pattern A of 25-percent 0-degree, 50-percent  $\pm 45$ -degree, and 25-percent 90-degree plies. The other, Pattern B, was stiffer in the wing bending direction and contained 37.5-percent 0 degree, 50-percent  $\pm 45$ -degrees, and 12.5-percent 90-degrees. Both of these patterns had been located on the plateau of maximum bolted joint efficiency reported in earlier testing [1]. Each laminate has a similar strength at bolt holes because the additional 0-degree fibers in Pattern B give a strength increase which is virtually nullified by the increase in the stress concentration factor associated with the deviation from isotropy. This relative insensitivity of the joint strength to the precise laminate pattern (throughout that range) affords the option of some juggling of wing bending and torsional stiffness to improve flutter characteristics. This eliminates the need for using different patterns in the vicinity of the bolt holes than remote from them. It is interesting to note that in an independent investigation of a fiber pattern for a composite wing in Europe, a building block of two 0-degree (spanwise) plies, four  $\pm 45$ -degree plies, and one 90-degree (chordwise) ply was selected. That is nearly in the middle of the range covered here.

Test laminate balanced layup sequences provided 0-degree fibers at the surfaces of all parts to facilitate the load transfer to bonded doublers in the grip area of the specimens. Changes of only  $\pm 45$  degrees were allowed between interior plies. There were no stacked plies except at the midplane of the 24-ply Pattern B laminate (with 8-ply unit sequencing). These constraints on the possible layup sequences are based on the need to avoid inducing microcracks at the interface between stacks of plies, as shown in Figure 3. Such microcracks are known to cause edge delamination problems with stacks of four or more 0.005-inch plies in brittle 350°F cured resins. Such edge delaminations impose a reduction in static compression allowable strengths as well as a drastic shortening of the fatigue life under tensile loading. Any such thermally induced delaminations around bolt holes are considered undesirable because, in contrast with the self-stabilizing mechanically induced delaminations, the former delamination continues to grow indefinitely under cyclic loads of sufficient intensity.

### 3. ANCILLARY TESTS

In the first phase of the test program, there were 180 ancillary test specimens having only one bolt hole. These tests covered loaded and unloaded holes, tensile and compressive loading, and three bolt sizes — 1/4 inch, 1/2 inch, and 3/4 inch. Most joints were loaded in double shear, but sufficient tests were also run in single shear to establish any differences. The tests were conducted to demonstrate the ability to predict the behavior of large, complex bolted joints, so the testing was not as comprehensive as it would be for a certification program. Earlier work indicated that pin-loaded joints fail at significantly lower average bearing stresses, about 50 percent of the strength for finger-tight nuts and bolts [1]. Likewise, subsequent testing at NASA showed that joint strengths are increased by torquing the bolts tighter (see Crews [5]). Also, tests on single-shear flush fasteners would be needed over quite a large fraction of the exterior skin. Any of these other effects could be incorporated in the present analysis for load-sharing once the pertinent test data have been acquired.

The ancillary tests generated complete load deflection curves to failure, characterizing both the linear and nonlinear regimes. A typical tensile load deflection curve for a bolted joint is shown in Figure 4. The failure in this case was in bearing because of a large width-to-diameter ratio (w/d) of 8.

RESIN COEFFICIENT OF THERMAL EXPANSION LARGE AND POSITIVE  
FIBER COEFFICIENT OF THERMAL EXPANSION VIRTUALLY ZERO

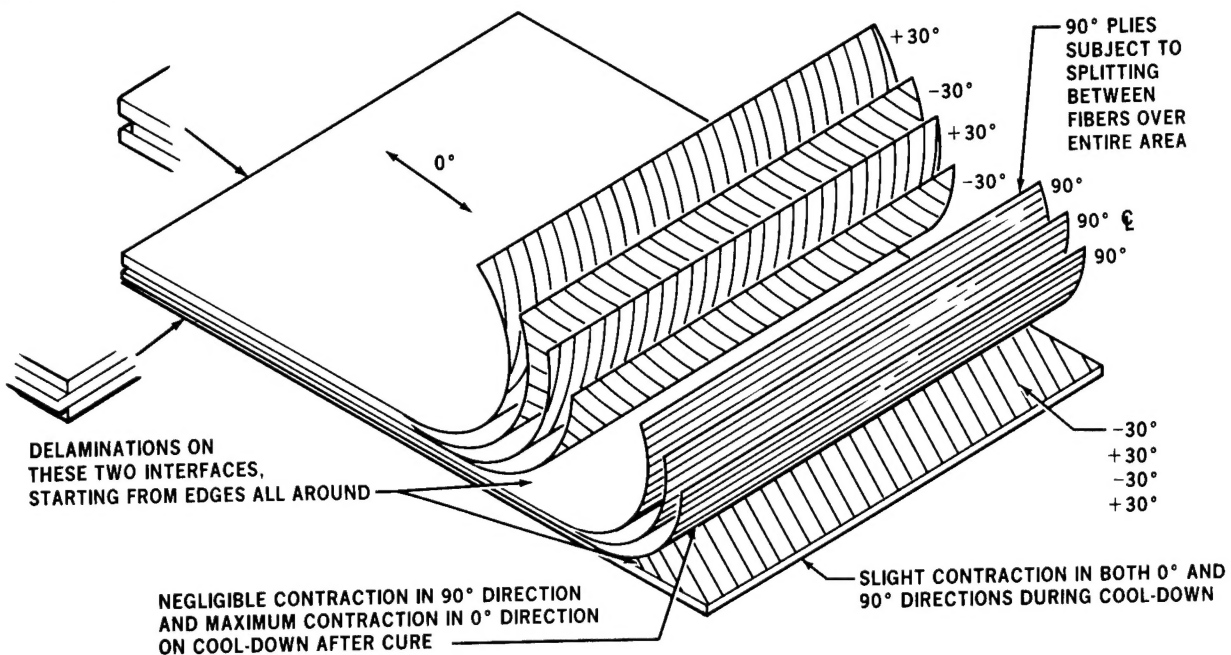


FIGURE 3. DELAMINATIONS OF COMPOSITES WITH BUNCHED PLIES INSTEAD OF INTERSPERSION

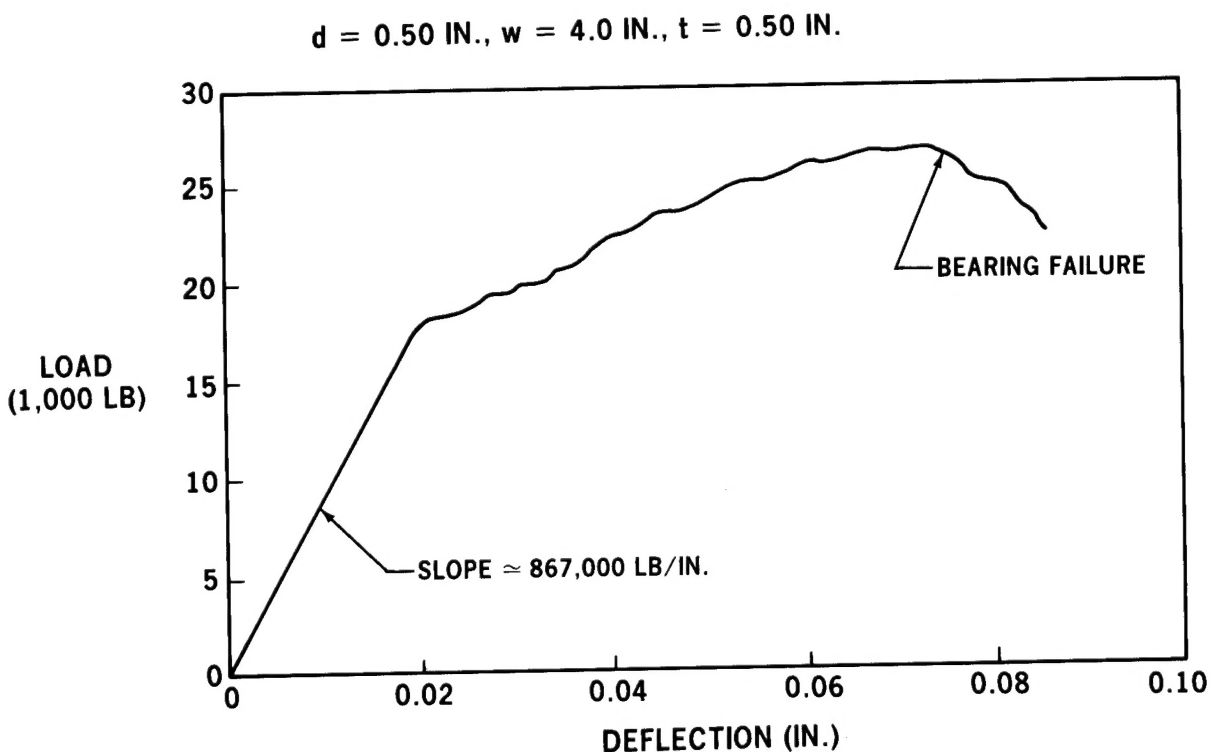


FIGURE 4. LOAD DEFLECTION CURVE, DOUBLE-SHEAR TENSION TEST (BEARING FAILURE)

Even the tension-through-the-hole failures were associated with quite high bearing stresses (80 to 90 ksi versus an ultimate value of 100 to 120 ksi) and, in the case of the 1/4-inch bolts, there was substantial bolt bending prior to failure. The nonlinear behavior permits the most highly loaded bolts in a joint to sustain their load without failure, while other more lightly loaded bolts can accept more load due to the added deformation at the critical bolts.

Some of the narrower strips ( $w/d = 3$ ) which were designed to fail in tension exhibited much less nonlinear behavior, as depicted in Figure 5. (In every case tested, the edge distance was sufficiently large to preclude premature failures by shear-out.) The significant nonlinear behavior associated with the nominally tensile failures, which were expected to fail abruptly, arose from one or two sources.

$d = 0.50$  IN.,  $w = 1.50$  IN.,  $t = 0.50$  IN.

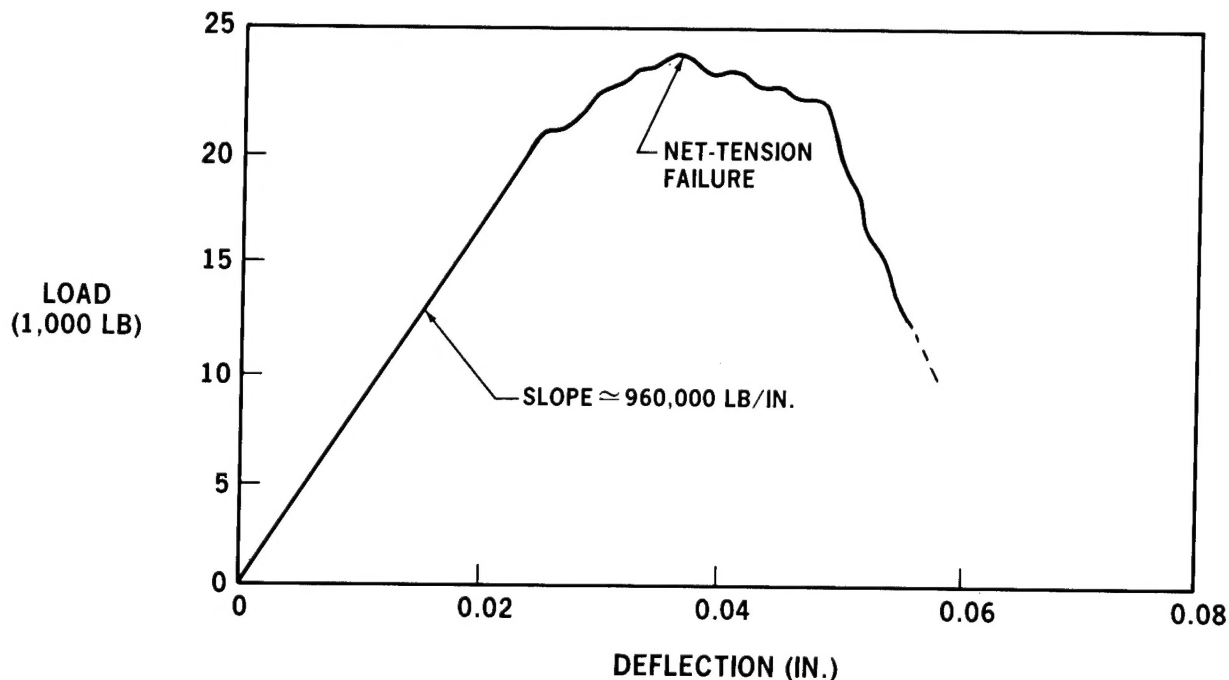


FIGURE 5. LOAD DEFLECTION CURVE, DOUBLE-SHEAR TENSION TEST (TENSILE FAILURE)

It was found that the linear portions of these load deflection curves could be represented accurately by minor modifications of an old NACA formula [4]. This is shown in Figure 6 for double shear, giving excellent correlation with the mean values, despite the large experimental scatter, the reason for which is not known. The stiffness formula is given as the sum of four components. Thus,

$$\frac{1}{K} = \frac{2\delta}{P} = C_{bs} + C_{bb} + C_{b_{br}} + C_{p_{br}}$$

Here,  $\delta$  is the deflection of the bolt in inches,  $P$  is the double-shear bolt load in kips, and the various contributions to the bolt constant (or flexibility) in inches per kip are  $C_{bs}$  for shear deformation of the bolt,  $C_{bb}$  for bending deformation of the bolt,  $C_{b_{br}}$  for the bearing deformation of the bolt, and  $C_{p_{br}}$  for the bearing deformation of the laminates or plate. The empirical expressions deduced by Tate and Rosenfeld [4] for this expression give, for bolts loaded symmetrically in double shear,

$$\frac{1}{K} = \frac{2t_s + t_p}{3G_b A_b} + \frac{8t_s^3 + 16t_s^2 t_p + 8t_s t_p^2 + t_p^3}{192 E_{bb} I_{bb}}$$

$$+ \frac{2t_s + t_p}{t_s t_p E_{b_{br}}} + \frac{1}{t_s (\sqrt{E_L E_T})_s} + \frac{2}{t_p (\sqrt{E_L E_T})_p}$$

in which the first subscript b refers to the bolt and the second to bending, s refers to each of the splice straps (which are assumed to be identical), and p to the basic plate (or skin). The various thicknesses are given by t, as shown in Figure 7, and the various elastic moduli are signified by E for a Young's modulus and G for the shear modulus of the bolt, which has an area  $A = \pi d^2/4$  and section modulus  $I = \pi d^4/64$  since d is the bolt diameter. The laminate moduli  $E_L$  and  $E_T$  refer to the longitudinal (or load) direction and lateral (or transverse) direction, respectively, and would be identical for quasi-isotropic laminates. These laminate moduli represent the only change from the original expression which used the moduli  $E_{sbr}$  and  $E_{pbr}$  instead.

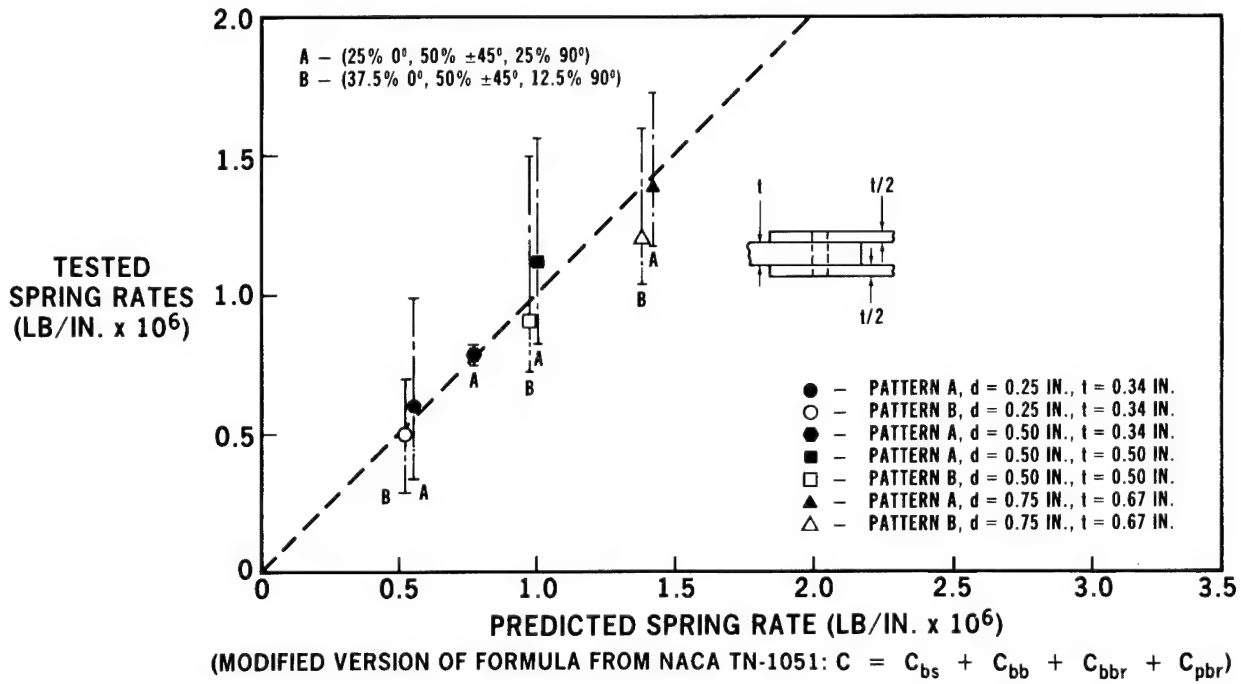


FIGURE 6. BOLTED JOINT ELASTIC SPRING RATES – TEST VERSUS PREDICTION

Figure 6 indicates that the orthotropic laminates (Pattern B) were predicted to cause almost the same effective bolt flexibility as for the quasi-isotropic laminates (Pattern A) and that, despite the greater fraction of longitudinal fibers in Pattern B, the test results showed that the bolted joints were actually slightly stiffer in the quasi-isotropic laminate A. The combination of this greater flexibility at the bolt holes in laminate B and the greater stiffness of that laminate between the fasteners should make it possible to develop a slightly higher strength in multirow bolted joints than could be achieved with the quasi-isotropic laminate A, but the net difference would not be substantial.

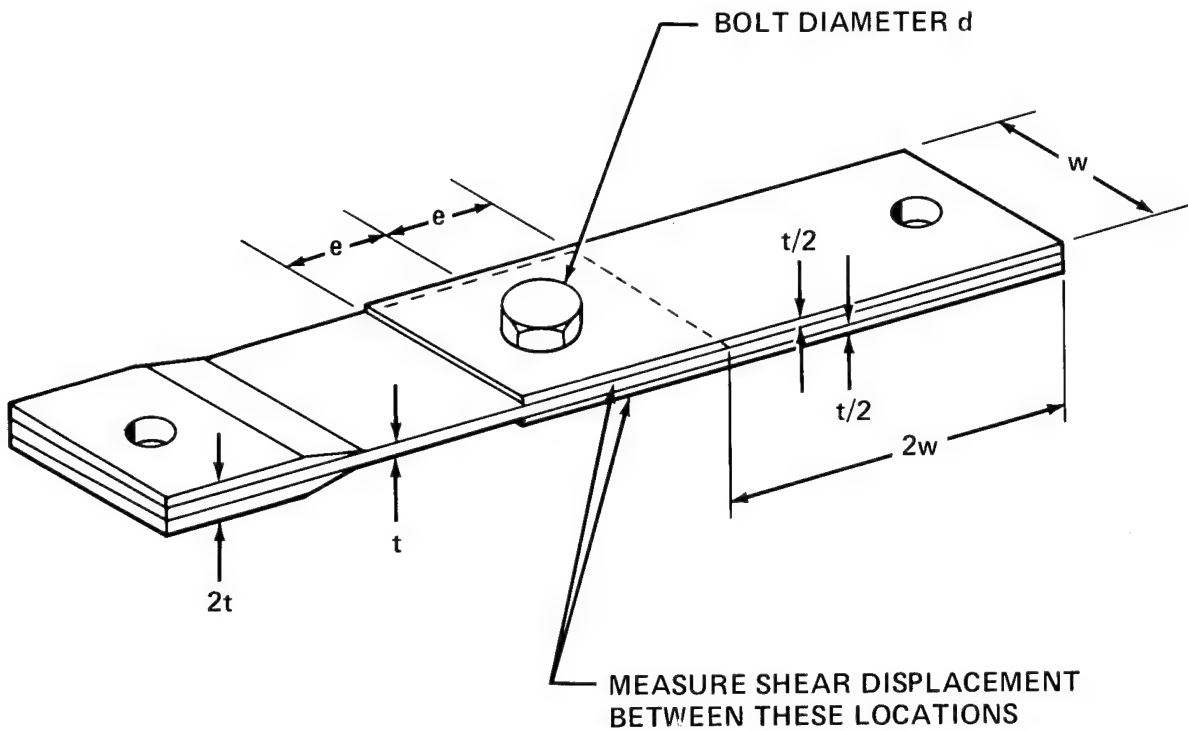


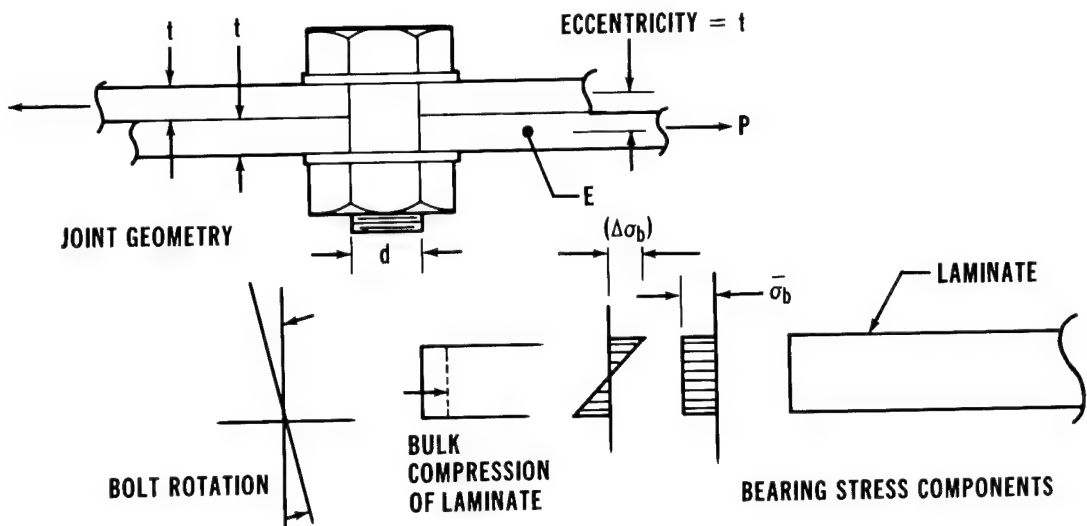
FIGURE 7. ANCILLARY TEST SPECIMEN – DOUBLE-SHEAR TENSION

All attempts to interpret the stiffness data for the single-shear tests in terms of existing formulas for metal joints failed. So the double-shear formula [4] was modified to account for the bolt rotation that occurs in single-shear joints. The first term, representing the shear deformation of the bolt, was taken to be unaltered. The second term, accounting for bolt bending, was deleted and the remaining three terms were all multiplied by the factor  $(1 + 3\beta)$ , where  $\beta$  represents the fraction of the bending moment on the bolt that is reacted by the nonuniform bearing stresses across the thickness. This is explained in Figure 8. The remaining fraction  $(1 - \beta)$  is reacted by the head and nut on the bolt. Therefore,  $\beta$  would vary from a maximum value of 1.0 for a simple shear pin, through a value of about 0.5 for countersunk fasteners, to a small fraction for torqued bolts with protruding heads, becoming very small for the combination of large washers with a large diameter-to-thickness ratio. The interpretation of the data from these tests, with a  $d/t$  ratio of about 2 and relatively small washers, indicates that  $\beta$  is on the order of 0.15 here. The need for the correction factor  $\beta$  arises because, as the fasteners rotate under single-shear loading, the bearing stresses become more concentrated near the interface between the members than is the case with double-shear loading. Consequently, the relative motion is increased by those locally higher bearing stresses.

The joint flexibility in single shear is thus expressed by the relation

$$\frac{1}{K} = \frac{\delta}{P} = \frac{2(t_1 + t_2)}{3G_b A_b} + \frac{2(t_1 + t_2)}{t_1 t_2 E_{b,br}} + \frac{1}{t_1 (\sqrt{E_L E_T})_1} + \frac{1}{t_2 (\sqrt{E_L E_T})_2} \quad (1+3\beta),$$

in which the subscripts 1 and 2 identify the two members. Figure 9 compares the stiffness predictions of this formula with the measured results. Had the  $\beta$  term not been included, the stiffness would have been overestimated by about 50 percent.



$$\text{BASIC MOMENT} = Pt = \bar{\sigma}_b dt^2$$

$$\text{INCREMENTAL MOMENT} = \beta pt = (\Delta\sigma_b)dt^2/3, \text{ COUNTING BOTH MEMBERS}$$

$$\text{BASIC RELATIVE DEFLECTION} = \frac{2\bar{\sigma}_b d}{E} = \frac{2P}{Et}, \text{ COUNTING BOTH MEMBERS}$$

$$\text{ADDITIONAL RELATIVE DEFLECTION} = \frac{2(\Delta\sigma_b)d}{E} = \frac{6\beta P}{Et}, \text{ COUNTING BOTH MEMBERS}$$

$$\text{RATIO OF TOTAL TO BASIC RELATIVE DEFLECTION} = (1 + 3\beta)$$

FIGURE 8. ADDITIONAL DISPLACEMENTS DUE TO BOLT ROTATION

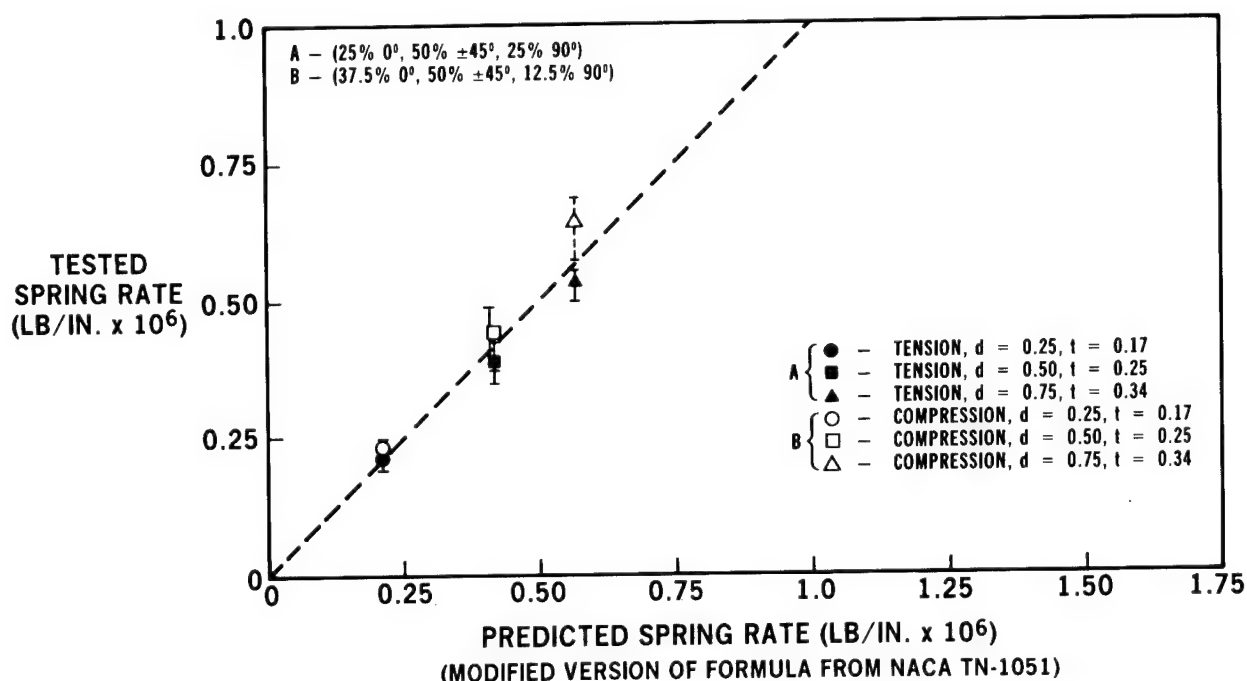


FIGURE 9. SINGLE-SHEAR BOLTED JOINT ELASTIC SPRING RATES – TEST VERSUS PREDICTION

The nonlinear portions of the load deflection characteristics influence the load-sharing in a multirow bolted joint only after some initial damage has occurred around the most critically loaded fastener, so the precision needed for that part of the analysis is less than for the linear analysis. However, it is important to represent the end of the linear elastic behavior accurately and to distinguish between the "brittle" or "ductile" behavior which may follow. Those effects are the key to any possible load redistribution. No universal formulas have been derived to express the nonlinear portion of Figure 2. Nevertheless, many analyses have confirmed that two simple rules cover most practical joint geometries. The first is that there is no significant nonlinear behavior for unloaded bolt holes.

The other is that the knee in Figure 2 can be located at about 80 percent of the ultimate failing stress in bearing. The secondary stiffness can be taken to be 20 percent of the elastic stiffness. The validity of these approximations was shown in the ancillary tests. When there is significant nonlinear behavior, particularly for the larger w/d values, the relative motion between the members is so great as to be unacceptable for design purposes, so it is useful to then add a displacement cutoff at 2 percent of the fastener diameter, just as for bolted joints in metal alloys.

The actual predictions of the test results for the multirow bolted joints were based on the stiffness formulas for the elastic behavior, with the definition of the nonlinear behavior taken from the actual load deflection curves from the appropriate single-hole tests because there was often considerable deformation prior to failure.

One significant finding of the single-hole tests was that, in double shear, the allowable strength of the central plate was always greater than that of the splice plates despite the matched thicknesses, presumably because of the better clamp-up. Therefore, in analyzing such joints, this extra strength should be accounted for in the input data. Such data would be necessary to truly optimize the design of such joints. The undamaged central plates should be retested with stronger splices because, in this test program, most of the failures occurred in the splice plates. This usually prevented the ultimate load capacity of the basic skins from being measured in the joint areas. The few test failures of the skins suggest that the additional bearing strength is an increment of about 20 percent. That correlates well with the measured bearing strengths in which fibrous composite skins were sandwiched between steel splice plates.

In addition to generating stiffness data, the ancillary test program provided the data for generalizing the measured section strengths at the bolt holes. Joint geometries were selected carefully to establish both net-section strengths and bearing failures, under both tensile and compressive loads. The tension-through-the-hole failure data were acquired with a width-to-diameter ratio of 3.0 for loaded holes and 2.0 and 8.0 for unloaded holes.

The observed stress concentration factors at failure are shown in Figure 10 and related to the equivalent (geometric) elastic isotropic stress concentration factors (from formulas given in [1]). As in prior test programs, there is considerable stress concentration relief prior to failure in the fibrous composites. The linear relation

$$(k_{tc} - 1) = C (k_{te} - 1)$$

is used to characterize these results. The values of C so deduced are 0.26 for the quasi-isotropic Pattern A and 0.42 for the orthotropic Pattern B. These are almost precise matches with Hart-Smith's measurements for graphite-epoxy composites [1], which adds considerable confidence in the use of this approach to generalize test results. Unfortunately, several of the test coupons failed in the doublers at the load introduction holes instead of the test area. Therefore, it was not possible to characterize the influence of the bolt diameter on the coefficient C, which is anticipated to increase with bolt size. The reason for selecting a w/d ratio of 3 for the loaded holes is that this value had been identified in prior tests as the geometry associated with the maximum strength of single-row bolted joints in graphite-epoxy composites. A value of 8 for the bearing tests was selected to ensure that there would be no interaction with the tension-through-the-hole failure mode. The edge distances,  $e$ , were made equal to the strip widths,  $w$ , to preclude shear-out failures.

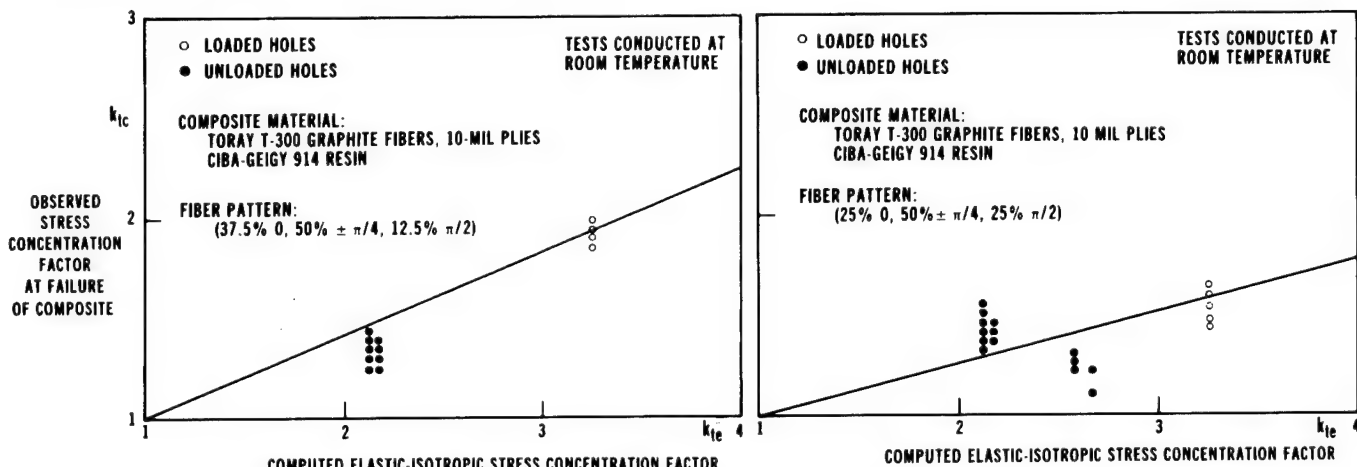


FIGURE 10. STRESS CONCENTRATION FACTORS AT FAILURE FOR COMPOSITE BOLTED JOINTS

The w/d ratios of 2 and 8 for the unloaded holes were selected with the intent of maximizing the range of values of elastic stress concentration factors,  $k_{te}$ . However, the narrow strips failed prematurely, in quite a different failure mode, with a clean tensile fracture rather than the massive delaminations associated with the wider strips. It is recommended that, henceforth, the minimum w/d ratio for unloaded holes be at least 3. Actually, since the bypass strength is needed primarily for multirow joints, for which the optimum w/d is in the range of 4 to 5 rather than the closer pitch of 3 for single-row joints, a case can be made for an even higher minimum w/d ratio. The unloaded hole results included in Figure 10 clearly show the different behavior for the narrow strips, in the form of abnormally high stress concentration factors  $k_{tc}$ . Some wider specimens of Pattern A were necked down slightly to a w/d of 6 in order to prevent failures in the grip areas. The unloaded hole tests demonstrated similar gross-section strengths at failure for both patterns at the w/d ratio of 8. At the w/d ratio of 2, the orthotropic Pattern B developed about 50 percent more strength than Pattern A. That strength ratio is about the same as the relative numbers of 0-degree plies in each laminate.

The unloaded-hole test results for compression were quite similar to the equivalent values for tension. Similarity also was evident in the loaded-hole tests. The gross-section failure stresses were on the order of 30 ksi for both patterns, with w/d = 3, while the ultimate bearing stresses were on the order of 100 ksi for both patterns for the wider strips (w/d = 8).

The great majority of the single-shear tests failed in bearing, at a stress of about 100 ksi, for both tensile and compressive loading. The w/d ratio of 8 was used throughout the single-shear tests. A special test fixture allowed the bolts to rotate, as they would on a wing spar, for example, but prevented the abnormal rotation of the laminates which would have occurred in a standard single-lap test coupon.

The basic unnotched laminate properties, used as a reference to establish the stress concentration factors  $k_{tc}$ , were measured as follows:

Pattern A:  $E = 7.4 \times 10^6$  psi,  $F_{tu} = 68,350$  psi,  $F_{cu} = 69,100$  psi

Pattern B:  $E = 9.3 \times 10^6$  psi,  $F_{tu} = 94,830$  psi,  $F_{cu} = 97,300$  psi

#### 4. ANALYSIS OF MULTIROW BOLTED JOINTS

Before presenting the results of the multirow bolted joint tests, an explanation will be given of how the data on single-hole tests, which were generated by the ancillary test program discussed above, are used to analyze more complex joints. The key to the analysis used here is the nonlinear computer program A4EJ [2]. This program can predict the load-sharing between the fasteners both at the limit of elastic (linear) behavior and after the load redistribution associated with any noncatastrophic initial damage. An equivalent linear program, BJBLM, has been coded by McDonnell Aircraft Company, at St. Louis, based on the analysis in McCombs, McQueen, and Perry [6]. That program is used in conjunction with the BJSFM program [3] to compute limit loads.

The A4EJ program is an iterative Fortran IV digital solution for the load-sharing between multiple parallel springs (the fasteners) and also accounts for the linear or nonlinear stretching of the members between the fasteners as sets of springs in series. Thus, both equilibrium of forces and the compatibility of displacements are ensured.

Figure 11 describes the elements of the mathematical model. At each station, it is necessary to define the load deflection characteristics of the fastener, including the local deformation of the members, as shown in Figure 12. For the members, the elastic behavior of each member between adjacent stations must be defined. A station is located at each fastener and at each discontinuity in either member. A tapered splice plate is represented elastically as a series of steps, with a precise match of properties at each fastener station.

Strength cutoffs are also needed for the fasteners in shear and for the members under combined bearing and bypass loads at each fastener station. The total load in a member, at each station, is the sum of the bearing load at that particular fastener and the bypass load which is reacted at other fasteners. These terms are explained in Figure 13, which also characterizes the bearing-bypass interactions for both tensile and compressive loads. The program could easily be modified to express the load-sharing under in-plane shear, as with torsion loads on a wing, but the failure criteria under those bearing-bypass interactions have yet to be established. The bearing-bypass interactions for tension and compression can be either linear or kinked, depending primarily on the local w/d ratio, as shown in Figure 13. Narrow strips, or closely spaced bolts, fail in tension-through-the-hole for both bearing and bypass loads; however, wide strips exhibit a bearing stress cutoff. Compressive loads have two possible interactions,

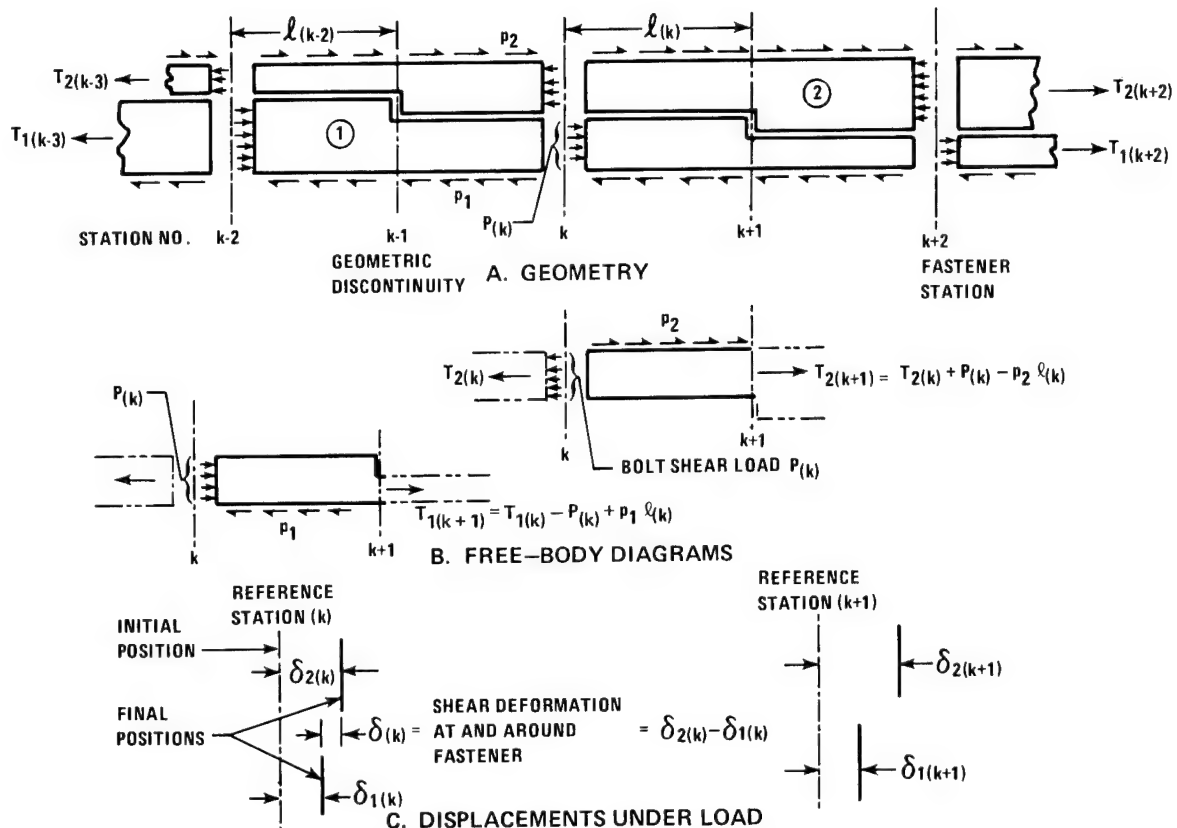
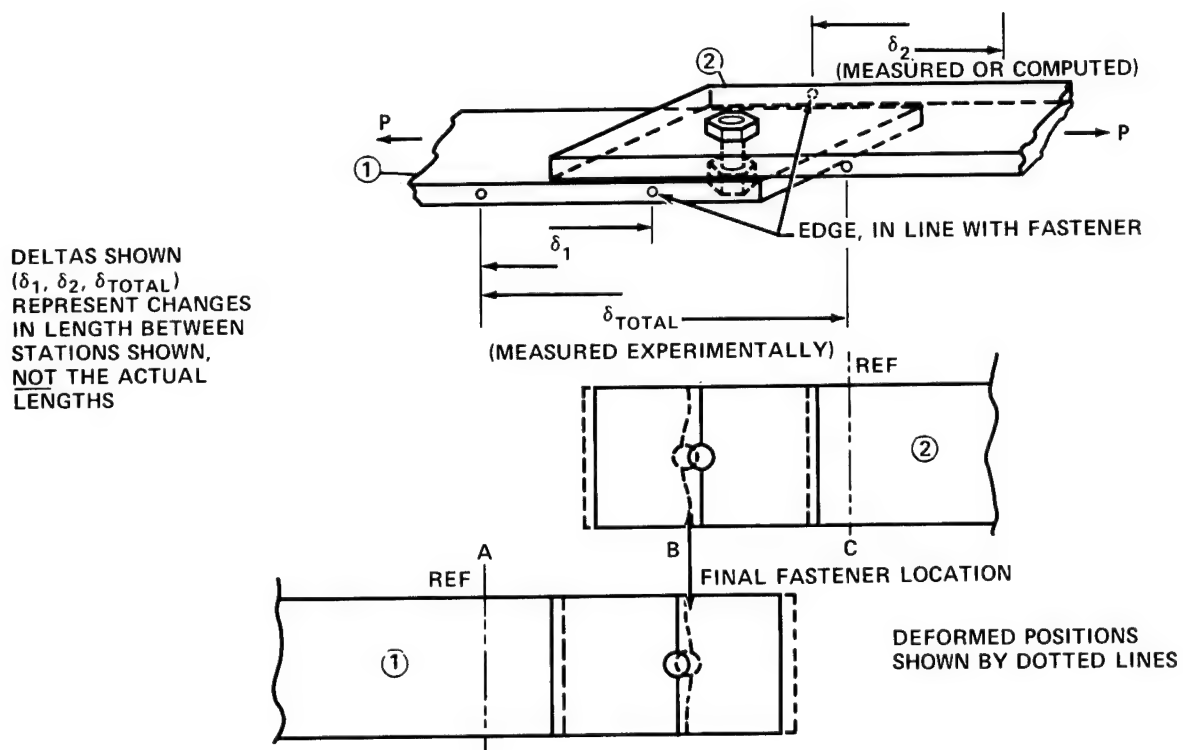


FIGURE 11. LOADS AND DEFORMATIONS ON ELEMENTS OF BOLTED JOINT



$$\text{EFFECTIVE FASTENER RELATIVE DISPLACEMENT} = \delta_{TOTAL} - \delta_1 - \delta_2$$

AND INCLUDES DISTORTION OF CROSS SECTION AT FASTENER STATION

FIGURE 12. DEFORMATIONS IN MECHANICALLY FASTENED JOINT

depending on whether the bolt fits tightly or loosely in the hole. In the case of a tight-fit hole, the combination of bearing and bypass stresses must not exceed the bearing allowable stress. With a loose-fit bolt, none of the bypass load can be transmitted through the bolt, causing a higher stress on the net section. In the case of a bolt hole with a very small clearance, the bolt may pick up a little bypass load as the composite laminate deforms under load.

The intercepts on the bearing-bypass interactions are established from direct experimental results or by means of the stress concentration formulas and relief given in Hart-Smith [1]. The following steps are involved in those calculations. First, the elastic-isotropic stress concentration factor  $k_{te}$  is calculated for both loaded and unloaded holes in tension. Those factors are reduced to the equivalent  $k_{tc}$  values via the reduction factor  $C$  to establish the actual intercepts. A bearing stress cutoff is added, if necessary, for wider bolt spacings. The same value of  $k_{tc}$  would be used for the compressive bypass strength at an unfilled hole and, in the absence of specific data for filled holes, a value half way between that  $k_{tc}$  and unity is recommended for filled holes under compression. The compressive bearing limit is self-evident. Usually, joints are more critical in tension than in compression, but the combination of high compressive bypass and bearing stresses may result in joints prone to widespread delaminations.

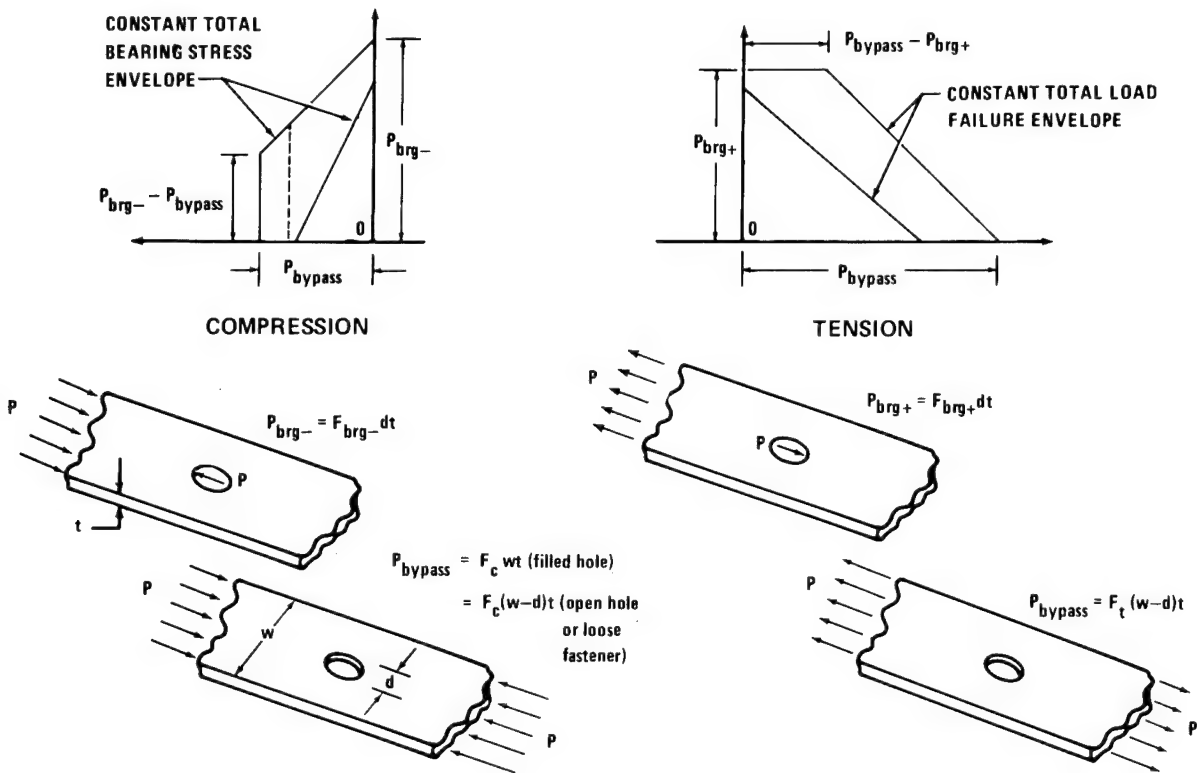


FIGURE 13. OUTER ENVELOPE OF BEARING-BYPASS LOAD INTERACTIONS

A further strength cutoff, that of failing the fasteners in shear, should never be an effective limit on joint strength. However, some designers of composite structures tend to use inadequately stiff fasteners in order to minimize their weight, on the basis of an apparent excess of shear strength. The consequences of such an approach are demonstrated clearly by the badly bent 1/2-inch-diameter bolts in Figure 14. As a rule of thumb, the bolt diameter should equal the thickness of the central member in a double-shear joint (or an individual splice plate if that is thicker), while for single-shear joints, the bolt diameter should be closer to the sum of the member thicknesses. Failure to abide by such rules results in excessive bolt bending, which causes more variation of the bearing stress across the thickness.

Worse, as a bolt which is too small bends, it relieves the through-the-thickness clamp-up on the composite laminate which, in turn, drastically reduces the bearing strength of the laminate on the surface. This results in delaminations at local bearing stresses as low as those for simple shear pins — only about half of the strength for torqued bolts of larger diameter. This phenomenon applies for both tensile and compressive loads, and is explained in Figure 15.

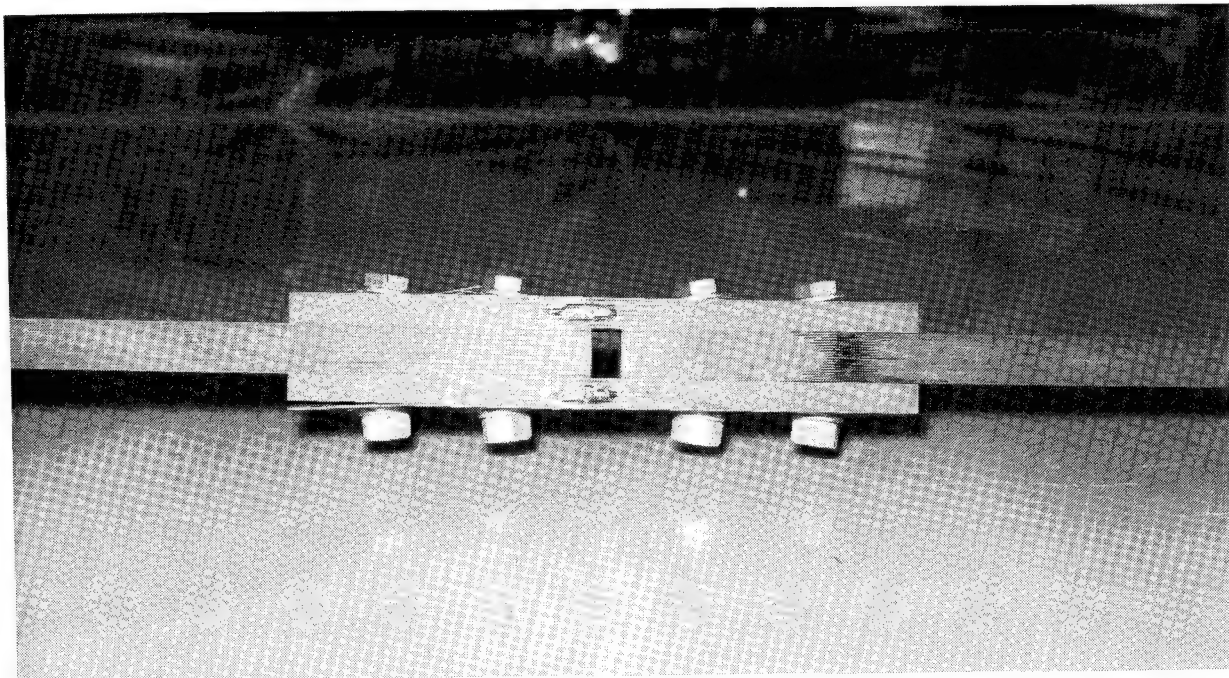


FIGURE 14. TWO-ROW BOLTED JOINT — NET-TENSION FAILURE WITH SEVERE BOLT BENDING

While on the subject of bolt bending, it is informative to compare the failure modes in Figure 14 and 16. Both specimens, JT24CF-503-1 and -2, were identical except for the nuts on the bolts. The larger (tension) nuts in Figure 14 provided much better clamp-up on the laminates and the failure was in net-section tension, with a little delamination, at the most critically loaded bolt hole. The bolts in Figure 16 had only shear-head nuts, two of which failed in hoop tension because of the tension load induced in the bolts by the severe bending. With the consequent loss of clamp-up on those bolts, they were then dragged through the splice plates, with the massive damage shown in Figure 16. The surface delaminations of the 0-degree plies on the outside of the splice plates, in line with the bolts at the other end of the joint in Figure 16, were observed in many tests. That suggests that the load in a 0.010-inch-thick 0-degree ply is too great to be sheared through a single resin interface, confirming the need to thoroughly intersperse all plies in laminates and to not stack parallel plies together.

In evaluating the load deflection characteristics of bolts in fibrous composite laminates, the elastic stiffness can be easily calculated on the basis of the formulas given above. The nonlinear behavior can be determined by the most critical possibility — the bearing or net-section failures of each member at that station or failure of the bolt in shear (or by yielding under bending).

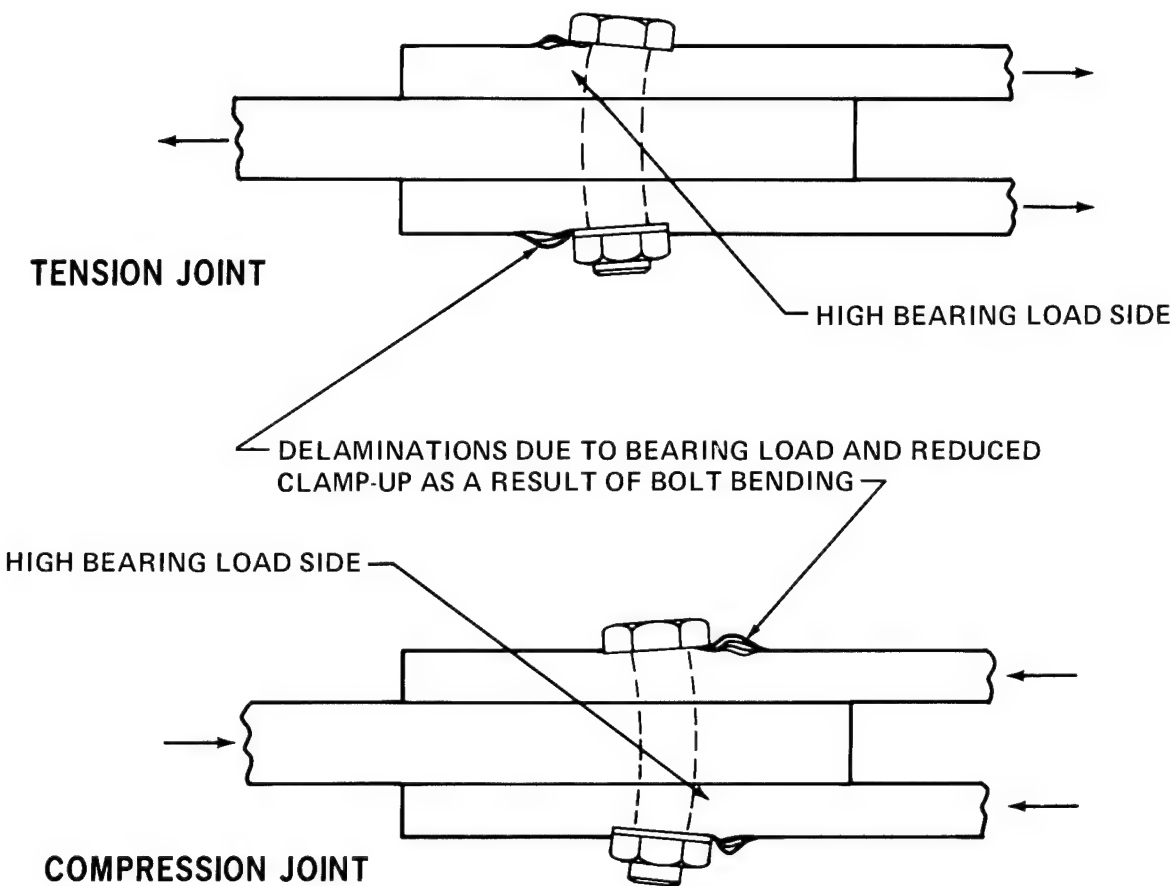


FIGURE 15. EFFECTS OF BOLT BENDING ON LAMINATE BEARING STRENGTH

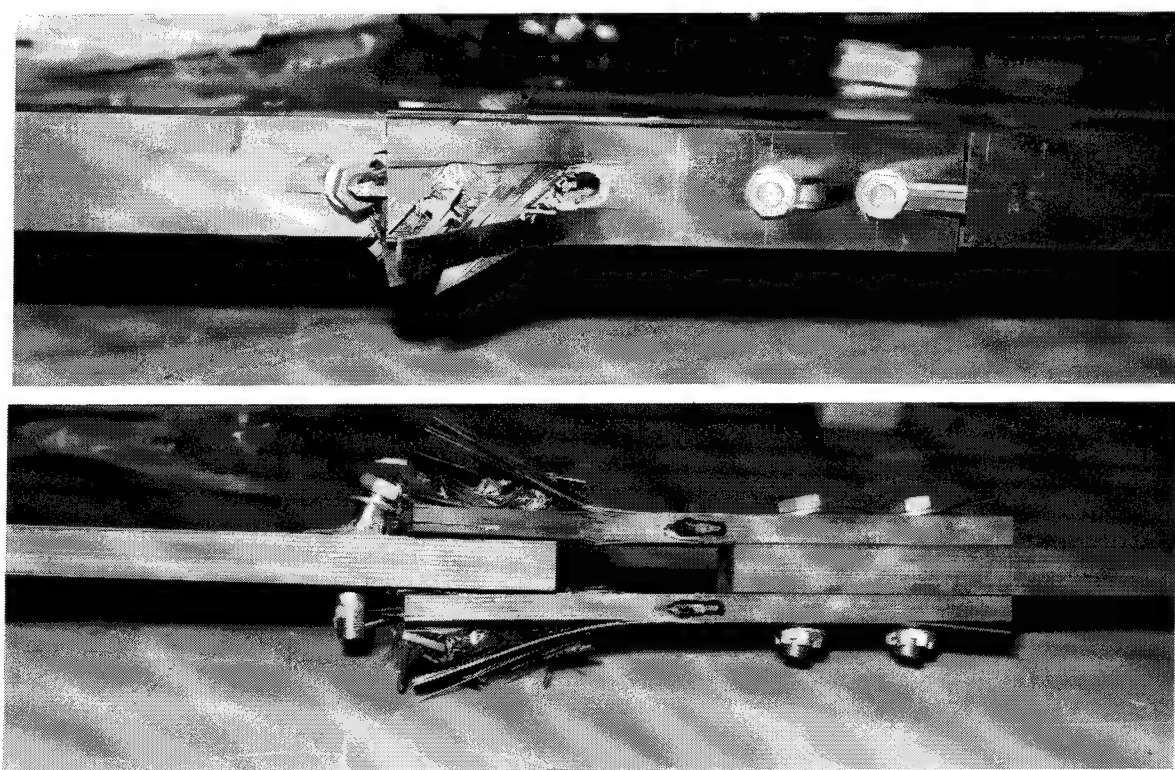


FIGURE 16. TWO-ROW BOLTED JOINT – BOLT FAILURE

## 5. OPTIMIZATION OF PROPORTIONS OF MULTIROW BOLTED JOINTS

Computer program A4EJ has been used to analyze and compare multirow joints of different concepts, as shown in Figure 17. Despite a natural inclination to expect the scarf joint to be the most efficient, it was actually shown to be the weakest, as well as the most difficult to manufacture and assemble. That conclusion should also be true for metal alloy constructions. The scarf joint failed basically because the thickness of the skin was reduced below nominal before the first fastener station was reached. (Obviously, one could counter that loss of area by a local buildup in the vicinity of the joint, but all of the concepts could be improved by the stress reduction associated with local reinforcement of the joint area.) It should be noted that the outermost rows of bolts in the scarf joints transfer less load than is carried by the interior bolts. That is caused by the reduced stiffness associated with local thinning of the skin and splice plates.

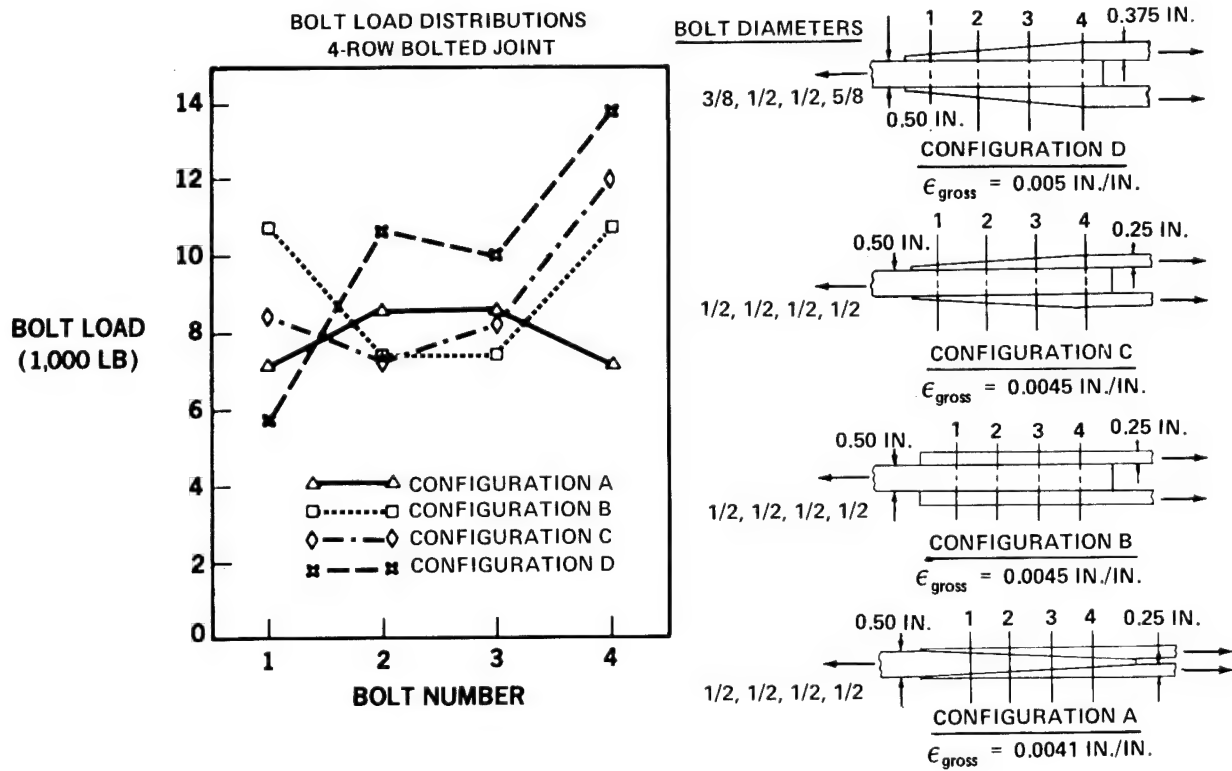


FIGURE 17. EFFECT OF JOINT CONFIGURATION ON BOLT LOAD DISTRIBUTION

The joint with uniformly thick splice plates was predicted to perform surprisingly well, and actually did in subsequent subcomponent joint tests. The combination of a uniform skin and reinforced tapered splice plates was predicted to be the most efficient joint design. Structural tests substantiated this result, despite premature failures as a result of delaminations in tapered splice members. The use of tapered washers rather than spot facing and an improved tapered splice design should eliminate this phenomenon and further verify the predicted superiority of this design. Nevertheless, in consideration of the interlaminar weaknesses associated with tapered members, the simple uniform joint should be looked upon as one of the two most viable candidate designs for fibrous composite construction. Certainly, the absence of critical interlaminar stresses, as in metallic construction, should make the joint with uniform skin and tapered splice plates the best candidate.

The use of tapered splice plates without reinforcement obviously cannot represent an improvement over the strength with uniform adherends since tapering transfers more load to the most critical fasteners, nearest to the middle of the splice plates where the skins butt together. Reinforcement of the tapered splice plates is needed not only because of the extra load transferred to those bolts but also because the splice plate joint allowables are weaker than those of the skin when the skin is sandwiched in double shear.

The superiority of the reinforced tapered splice members in combination with a uniform skin can be explained easily. The greatest strength is obtained by maximizing the total load at the outermost row of fasteners — that is, the first row of fasteners in the skin — and this involves decreasing the bearing load in order to maximize the bypass load, which represents the sum of all of the other bolt loads. This design philosophy is reflected in Figure 18, which shows that the only way a multirow joint can be more efficient than the optimum single-row joint is by minimizing the bearing stress and further separating the bolts. Normally, the two requirements would be contradictory, but the tapered splice plates permit this. If the tapering were excessive, so little load would be transferred by the first row of bolts that an excessive load would remain to be sheared by the last row in pure bearing, with no bypass load left. Normally, the intermediate bolts will always be less critical in the skin than the end bolts. The sequence of iterations in optimizing the design is governed by maximizing the total load (or gross-section strain) in the skin at the first row of fasteners while not causing a premature failure in either the skin or splice at the last row of fasteners. Since there is no bypass load in the skin at the last row of fasteners, it is desirable to maximize the load transfer there to relieve the load on the first row. Only local reinforcement is needed in the splice plates to tolerate the combination of maximum bearing and bypass loads. A larger diameter fastener for the last row of bolts or a smaller one for the first row, where the splices are thinnest, will often be of assistance in this optimization process. Any small extra weight in the splices or fasteners is worth incurring to maximize the efficiency of the large, heavy skins. It is wrong to evaluate splice efficiencies only on the basis of minimizing the weight of the splices and fasteners.

Figure 18 was prepared for the orthotropic Pattern B used in the subcomponent tests for this investigation. It is remarkably similar to Figure 26 in Hart-Smith [7], which was prepared for thinner tapes in the quasi-isotropic Pattern A. The higher modulus of the Pattern B laminates means a strength increase of about 25 percent with respect to the earlier joints tests on the Pattern A material.

At this point, a simple technique for the design of bolted graphite-epoxy structures, which has been used successfully in several hardware programs, will be assessed. While the precise numbers vary a little between projects and aerospace companies, the general form of the procedure is as shown in Figure 19. Some recent examples of this method may be found in Garbo [8]. A gross-section strain for unloaded holes (0.004 shown) is reduced linearly with the bearing stress on each bolt (down to 0.003 at a bearing stress of 100 ksi). The ends of that interaction are identified by the points A and B, which are shown in Figure 18 for a typical minimum w/d of 6 for spanwise seams of fasteners (aligned with the load direction). Such simple design rules are slightly conservative, but easy to apply in many situations without risk. Indeed, the only common area of risk is associated with the more highly loaded and more closely spaced bolts in a chordwise seam of fasteners (perpendicular to the load direction). Consequently, it is customary to add an allowable bearing stress cutoff to Figure 19, at about 50 to 60 ksi. The use of higher bearing stresses is not prohibited, but it is confined to a few situations in which the analysis is made to a sufficiently greater depth.

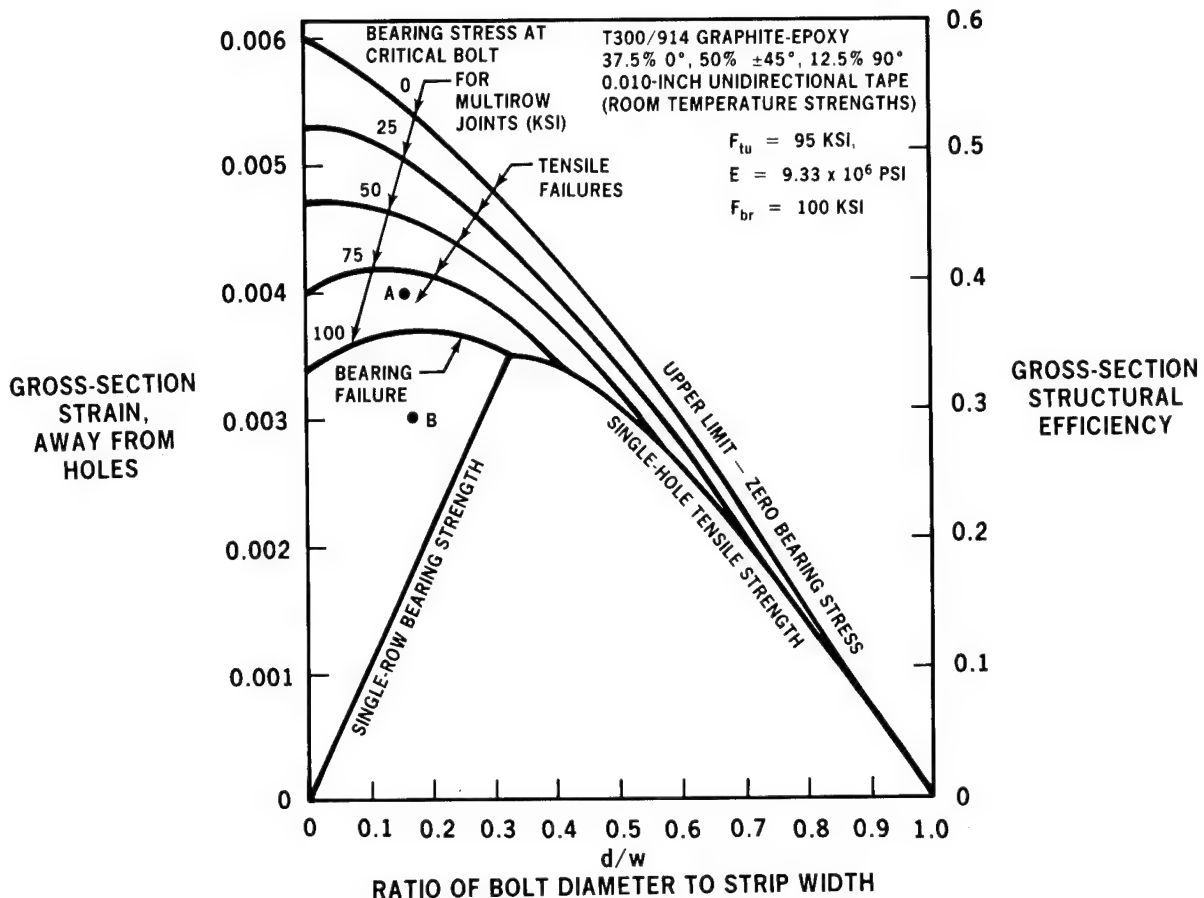


FIGURE 18. STRESS CONCENTRATION INTERACTIONS IN MULTIROW BOLTED COMPOSITE JOINTS

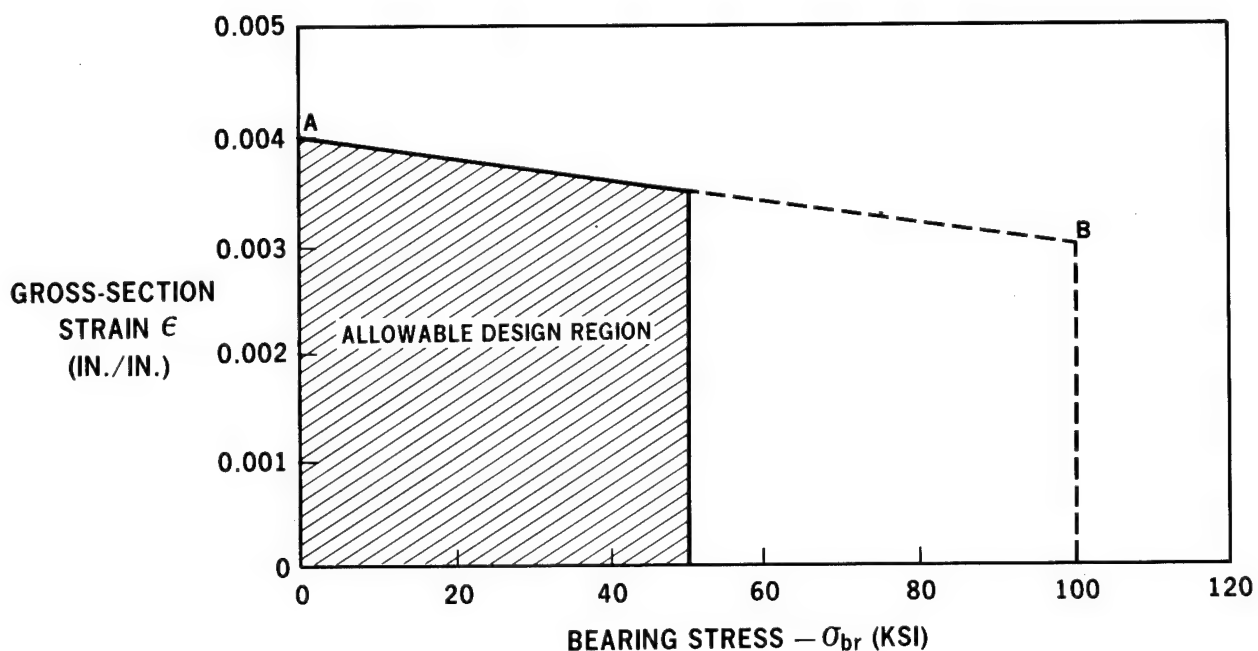


FIGURE 19. DESIGN TECHNIQUE FOR BOLTED GRAPHITE-EPOXY STRUCTURES

## 6. SUBCOMPONENT TESTS

The methods and data described above have been used to analyze in advance of testing the strengths of 20 larger multirow bolted joints. All of these test specimens were built with the orthotropic fiber Pattern B. This entire test series is described in Figure 20 and the full results are given in Bunin [10]. Certain features of that program are presented here to publicize the key features of the joint behavior and to illustrate the capabilities of the A4EJ computer program.

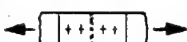
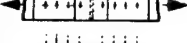
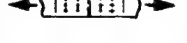
COMPONENT	LOAD TYPE	NO. OF SPECIMENS		SPECIMEN CODE	BOLTS PER SPECIMEN	d (IN.)	t LAM (IN.)	w (p) (IN.)	w/d (p/d)
		CLEARANCE FIT	INTERFERENCE FIT						
	TENSION	2	2	JT4CF IF JC4CF IF	4	0.500	0.832	2.15	4.30
	COMPRESSION	1	1						
	TENSION	3	1	JT8CF IF JC8CF IF	8	0.375/ 0.437	0.832	2.15	5.75/ 4.92
	COMPRESSION	1	1						
	TENSION	1	1	JT12CF IF JC12CF IF	12	0.750	0.996	9.00 (3.00)	(4.0)
	COMPRESSION	1	1						
	TENSION	1	1	JT24CF IF JC24CF IF	24	0.500/ 0.625	0.996	6.00 (2.00)	(4.0, 3.2)
	COMPRESSION	1	1						

FIGURE 20. SUBCOMPONENT TEST PROGRAM – SPECIMEN DESCRIPTION

The most notable highlight of the testing of these large bolted joints was the ability to consistently attain gross-section failure strains on the order of 0.005 in these room temperature tests for both tensile and compressive loads. Despite the additional reinforcement of the splice plates to stiffen them up and so modify the bolt load distribution favorably, most of the failures occurred in the splice plates rather than in the skins which, being in the middle of the sandwich, had greater allowable strengths. A frequent failure mode associated with the machine-tapered doublers was the delamination of the splice plates, as shown in Figure 21. The prime cause of that mode of failure was believed to be the spot facing for the bolt heads, nuts, and washers. Tapered washers would be preferred in the future. However, the possibility remains that the delaminations were initiated at small cracks on the surface due to machining, and it should be noted that such tapered laminates have been laid up and cured net by other investigators. Because of these unanticipated failures, which reduced the effective thickness of the splice plates, those specimens were reanalyzed and were then predicted to fail at the lower observed loads.

Another unanticipated form of premature failure concerned the bearing-bypass interaction under compressive loads. Some of the splice plates delaminated at many interfaces, as shown in Figure 22, across the area in which the skins butted together. (In contrast, the tensile delaminations began on the outer, or sloping, faces of the ends of the splice plates and were usually confined to one or two interfaces, as shown in Figure 21.)

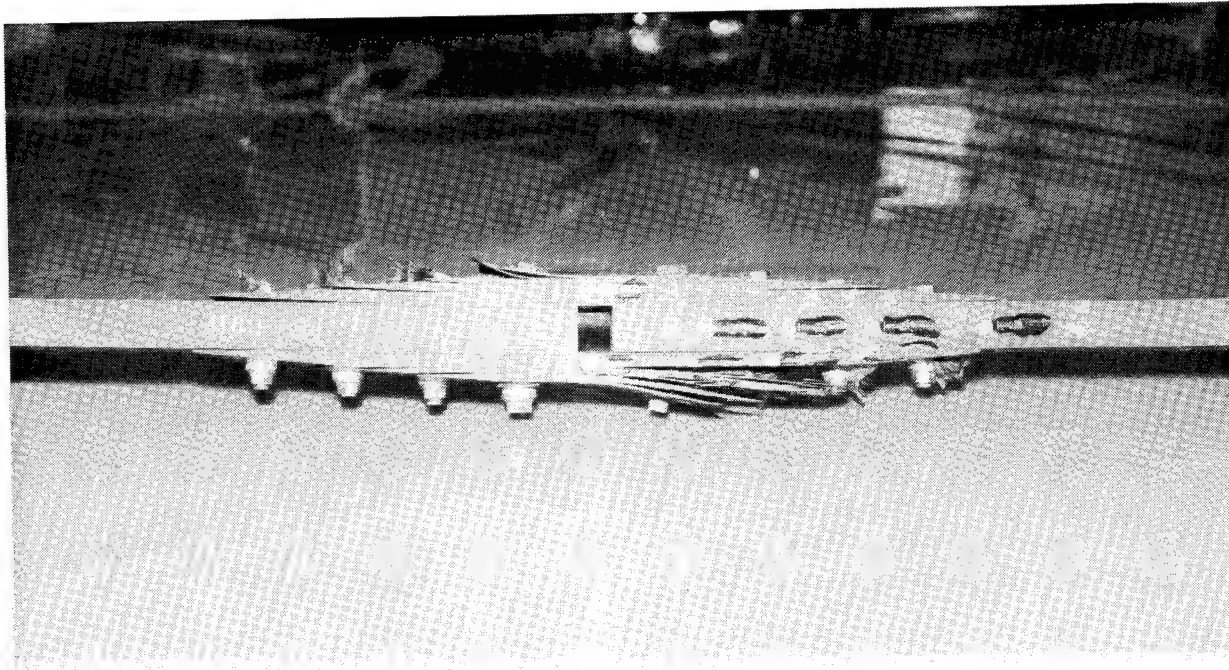


FIGURE 21. FOUR-ROW TENSION JOINT – SPLICE PLATE DELAMINATIONS

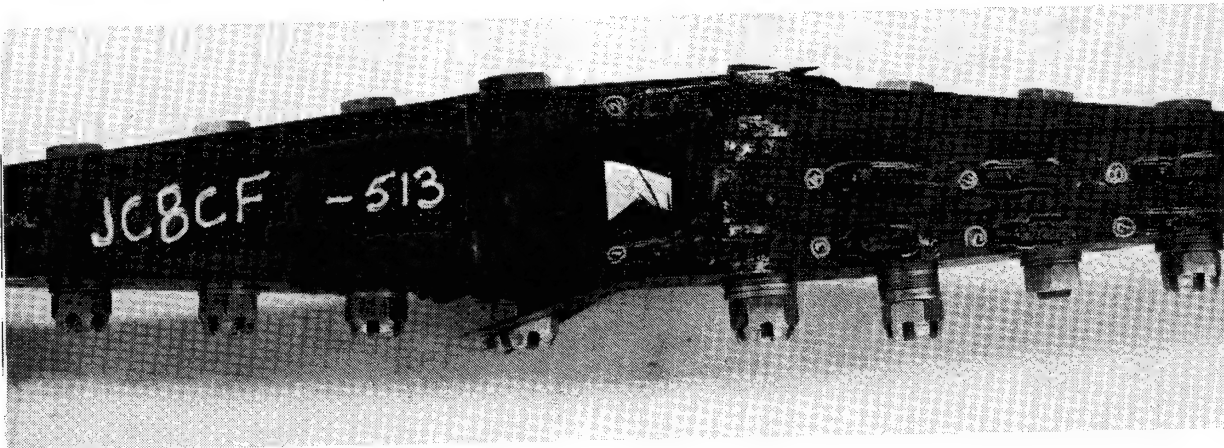


FIGURE 22. FOUR-ROW BOLTED JOINT – COMPRESSION FAILURE

The following explanation is offered for the premature compressive delaminations. When a single fastener joint fails in bearing, there is invisible but detectable damage starting at about 50 percent of the ultimate failure stress. Prior to failure, those small delaminations are self-stabilizing in the sense that an increase in load is needed to make them propagate. However, when the bearing stress trajectories around such a fastener are superimposed on a nominally uniform compressive bypass load, the initial delaminations seem to spread catastrophically. It should also be noted that as the bolts bent under their applied shear loads, as shown in Figure 15, the bolt heads and nuts moved away from the surface of the splice plates on the more highly loaded side of the bolts. That, on its own, would be sufficient to decrease the effective bearing stress allowables for at least the outer plies. It is clear that large pre-torqued bolts and even larger washers can be effective in maximizing the strength of bolted joints loaded in compression.

The first of the subcomponent tests to be described here is identified as JT12CF and contained six 3/4-inch-diameter bolts on each end of the splice plates, arranged in two rows. This double-shear specimen had a central plate thickness of 1.00 inch and splice thicknesses of 0.67 inch each. The total width across the three columns of bolts was 9.0 inches, giving a pitch-to-diameter ratio of 4, with an edge distance of 2.25 inches, for an  $e/d$  ratio of 3 and a separation between the bolts of 4 inches or 4d. Because the total thickness of the splice plates exceeded that of the skin, more load would be transferred at the outermost row of fasteners and the critical member would therefore be the skin and not a splice member.

Both the test result and the predictions confirm this. The joint strength at the critical location is limited by the bearing-bypass envelope shown in Figure 23, which also shows the excellent agreement between the test result and the predicted ultimate load. A tension-through-the-hole failure had been predicted, and that is consistent with the appearance of the failed specimen shown in Figure 24, with a clean textbook fracture. It should also be noted that the bearing load at that bolt row is greater than the bypass load which is reacted at the other row of bolts. The gross-section failure strain of 0.0042 in the skin is shown to match the prediction at point C in Figure 25 for a  $d/w$  ratio of 0.25 and a bearing stress of 70 ksi. The bearing stress cutoff in Figure 23 corresponds to a failure stress of 100 ksi. It probably should have been somewhat higher for a bearing strength of 120 ksi in the sandwiched member rather than the 100 ksi which would remain applicable for the less severely loaded skin. Nevertheless, that refinement would not alter the sloping line for the tension-through-the-hole failures and would therefore not affect the predicted failure load. The failure strain of 0.0042 is impressive for such a simple joint geometry, but Figure 25 indicates that still higher results should be attainable for more efficient joint geometries.

2-ROW, 3-COLUMN TENSION AND COMPRESSION SPECIMENS  
 $d = 0.75$  IN.,  $w = 9.0$  IN.,  $t_{\text{SKIN}} = 1.0$  IN.,  $t_{\text{SPLICe}} = 0.67$  IN. (x 2)

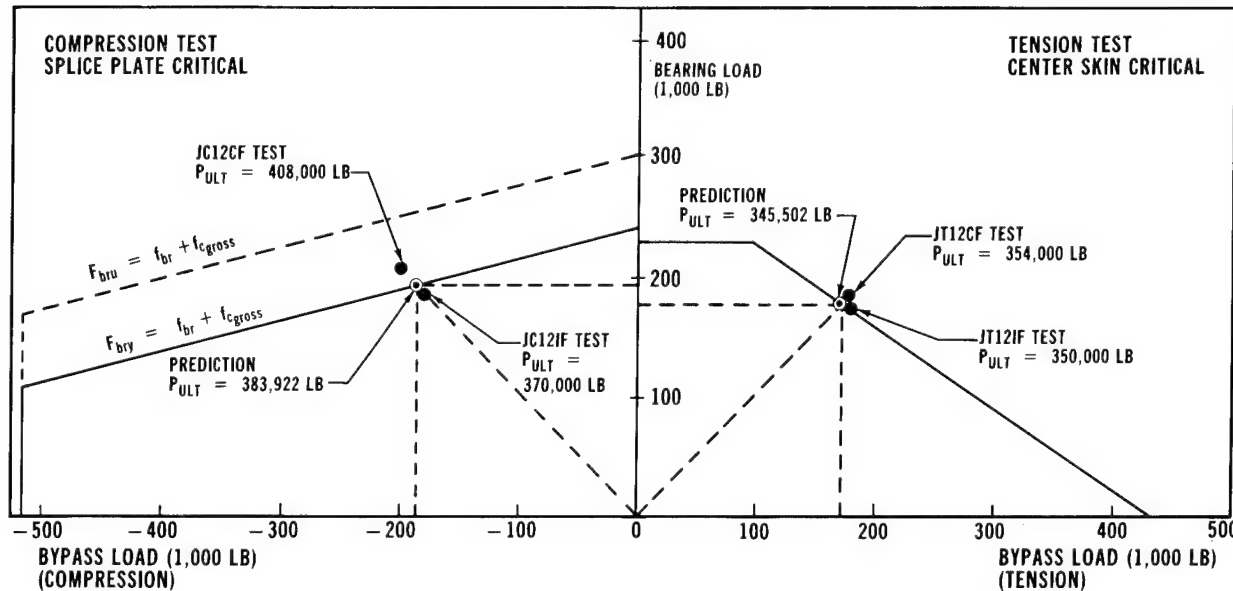


FIGURE 23. BEARING-BYPASS FAILURE ENVELOPES

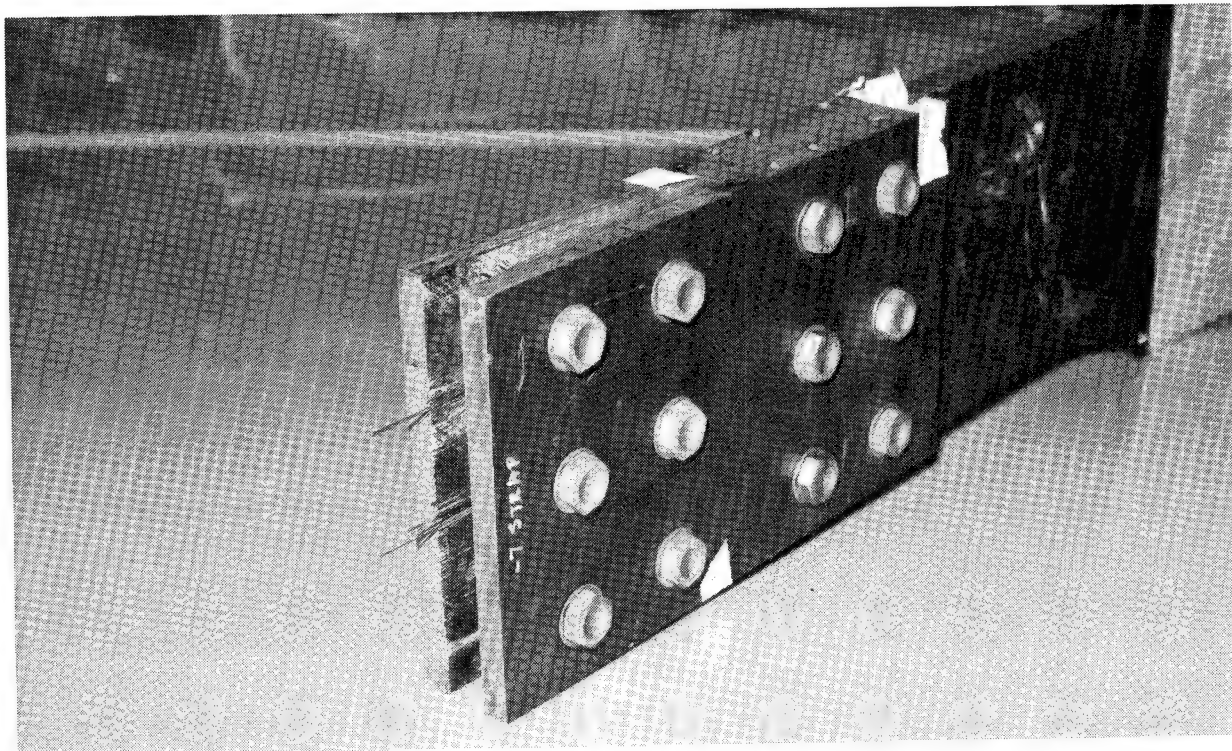


FIGURE 24. TWO-ROW, THREE-COLUMN SUBCOMPONENT JOINT – NET-TENSION FAILURE

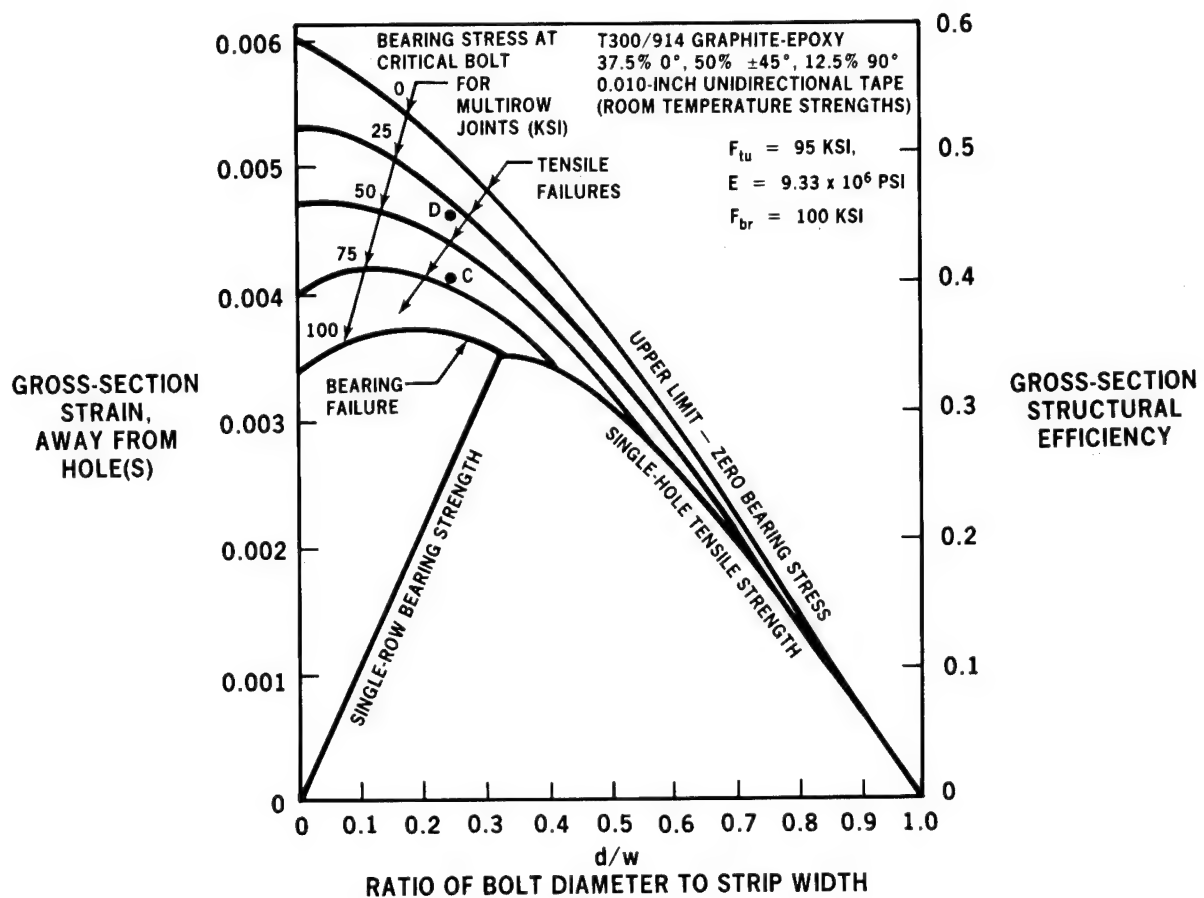
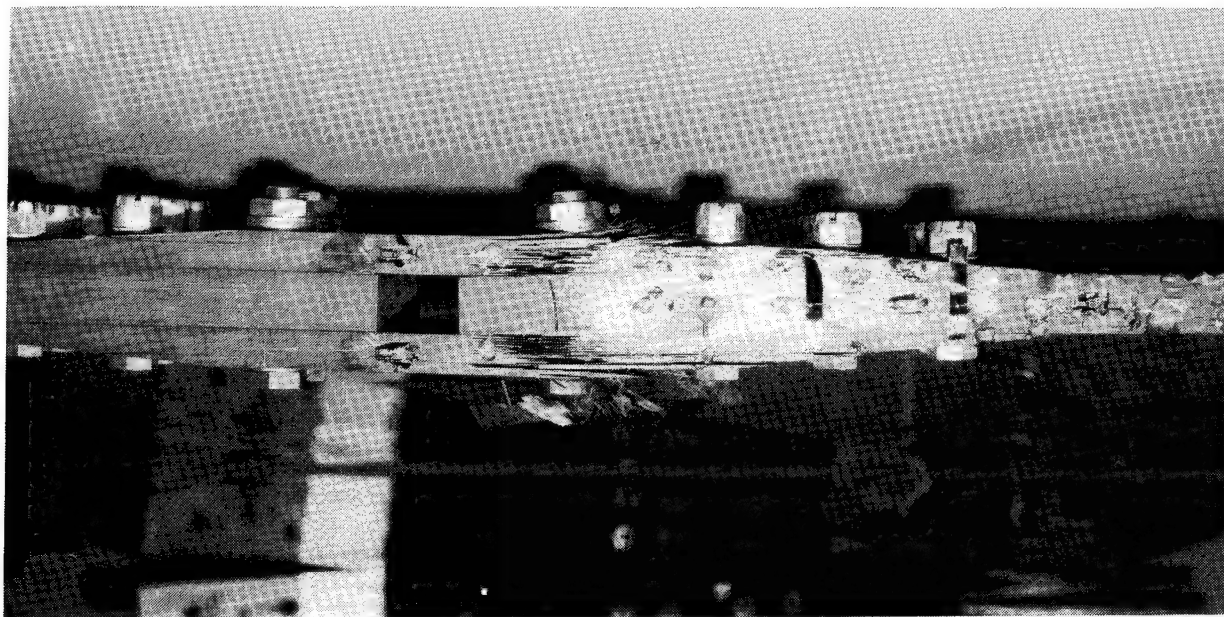


FIGURE 25. IMPROVED JOINT EFFICIENCIES FOR MULTIROW BOLTED COMPOSITE JOINTS

This potential for improvement is confirmed by test results D in Figure 25, obtained with the specimen JT24CF. This 24-bolt specimen had tapered splice plates with four rows of bolts at each end, in three columns. The total width was 6.0 inches and the thickness of the skin was again 1.0 inch. The maximum and minimum splice plate thicknesses were 0.67 inch and 0.08 inch, respectively. The failure load of 259,000 pounds corresponds with a gross-section strain of 0.0047 in the skin at the first row of bolts. The calculated bearing stress on these 0.5-inch bolts for this load was 30 ksi, indicating good agreement between test and theory at point D in Figure 25.

Actually, a slightly higher strength of 286,055 pounds, or a gross section strain of 0.0051, had been predicted. The test failure was, in fact, triggered by delaminations starting on the outside surface of the tapered splice plates, as shown in Figure 26. When one delamination propagated beyond the last row of the bolts to the middle of one splice plate, the effective thickness of that splice plate for carrying bypass load was reduced considerably. This resulted in an instantaneous secondary failure. The onset of the initial delamination has not been analyzed. In any case, it would be more fruitful to learn how to design joints not subject to that phenomenon, which is believed to have been induced by the spot faces at the bolt holes. Any future designs should use tapered washers under the bolt head and nut.



**FIGURE 26. FOUR-ROW, THREE-COLUMN SUBCOMPONENT JOINT – TENSION FAILURE AT REDUCED THICKNESS DUE TO SPLICE PLATE DELAMINATIONS**

This specimen used 5/8-inch-diameter bolts for the last row in the skin, with the objective of stiffening them up to accept more load — the reinforced splice plates were not predicted to be critical — and to decrease the bearing stresses there in all members. All the remaining bolts were of 0.5-inch diameter.

Several of the four-row subcomponent joint specimens, including JT24CF, were equipped with 18 strain gages mounted along the length of the joint on both sides of the central skin member and one splice member. These gages were located midway between the bolt rows. Additional gages were mounted away from the bolts in all three members to verify the lack of bending deformations. Strain

readings taken at predetermined increments where loads were applied to joints were used to calculate the bolt load distribution through the test. Analyses using the A4EJ program were run at the same load increments to solve for the joint internal loads in addition to the ultimate load solutions.

A comparison of the test and analysis results for this four-row, three-column joint is presented in Figure 27. The predicted loads were taken directly from the A4EJ solutions at each applied load level. The test data needed further interpretation because of the nonuniform strains across the widths of the specimen. All readings at any one station were adjusted by the same factor so that the sum of skin and splice plate loads would equal the joint-applied loads at any location along the joint. The transition from linear to nonlinear behavior due to bearing yield at the thin end of the splice plates is clearly observed at bolt row No. 1 in Figure 27. The observed higher bearing yield is possibly due to a much greater diameter-to-thickness ratio for these particular holes, in effect giving more clamp-up than in the tests for un-tapered specimens. In addition, the effects of the premature delaminations of the splice plate outer plies, which plagued all of the tapered splices during the tension tests, are also visible as sudden variations in load distribution at a joint with an applied load of approximately 200,000 pounds.

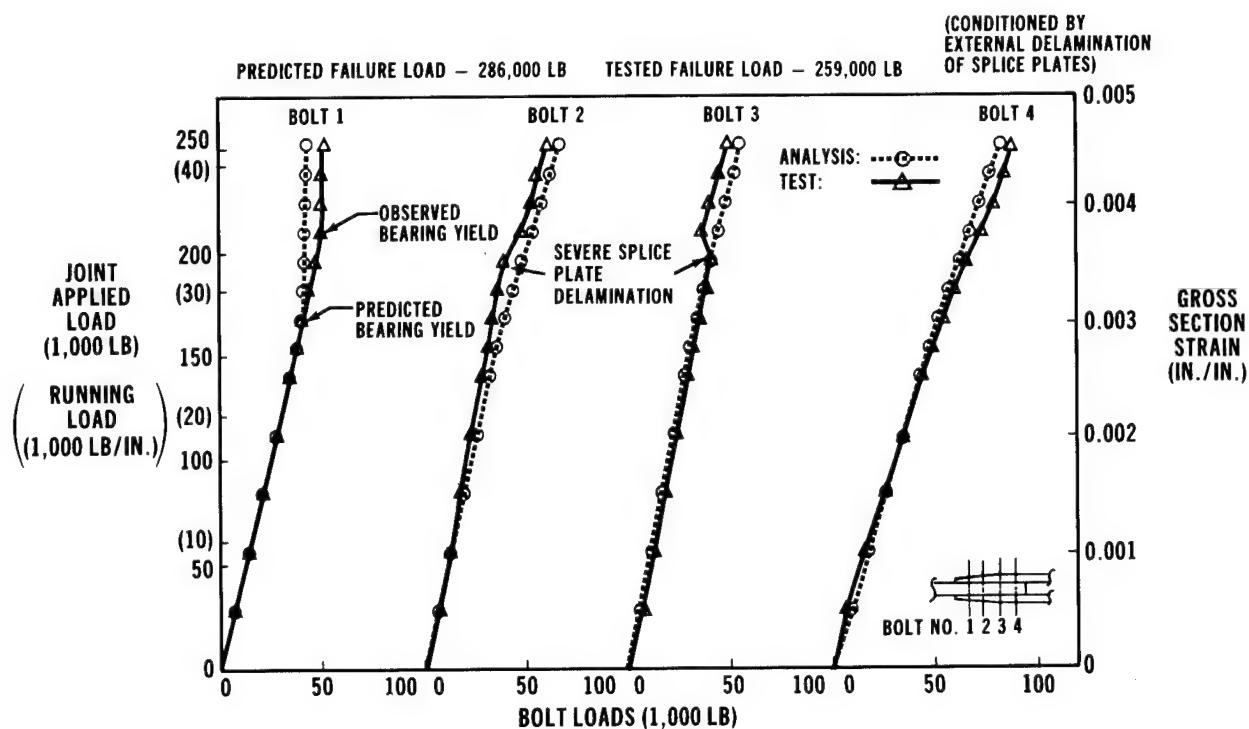


FIGURE 27. BOLT LOAD DISTRIBUTION - ANALYSIS/TEST CORRELATION

The tested failure load of 259,000 pounds occurred when a delamination originating at bolt row No. 2 propagated beyond the fourth row of bolts. This reduced by half the effective area of the splice members for carrying bypass loads at that most highly loaded row of bolts. A net-section tension failure followed instantaneously. Despite this difference in failure modes, the test specimen attained 90 percent of the predicted joint strength. The message from these tensile tests on tapered splice plates is that there are small but significant benefits to be realized by improving the detailed design or fabrication of such splices.

Geometrically similar test specimens, JT12IF and JT24IF, were tested with interference-fit sleeved bolts instead of the solid titanium bolts used in the two specimens discussed above. The first test did not accomplish its purpose, however, because the annealed sleeves in combination with smaller titanium bolts resulted in gross bolt yielding, at a load of 350,000 pounds, just under the 354,000 pounds sustained by the JT12CF specimen. The subsequent JT24IF test used steel instead of titanium for the core bolts and reached 265,000 pounds, a modest improvement over the 259,000 pounds for the clearance-fit titanium bolts in the JT24CF specimen. But, again, the comparison between bolt types was nullified by the delaminations of the splice plates. The similar comparisons under compressive loads were invalidated by the same problems of fastener yield for JC12IF and splice plate delaminations for JC24IF. It had been anticipated that the use of interference-fit fasteners should have increased the joint strengths because of improved load-sharing between the bolts. The analysis program A4EJ has been used to assess the load redistributions due to selective clearances around individual bolts in multirow joints [2].

Testing of similar multirow joints in compression established that these joints were stronger than when loaded under tension. This testing also showed that the allowable ultimate compressive bearing stresses may be severely restricted in the presence of high compressive bypass loads.

Good correlation between test and theory was found for the JC12CF and JC12IF specimens with two rows of 3/4-inch bolts. These specimens had uniform splice plates and three columns of bolts in each row, having the same geometry as the tensile test specimens described above. The test results of 408,000 and 370,000 pounds, respectively, closely agreed with the 383,922 pounds determined by analysis. These results are plotted on the left side of Figure 23, with the strength limited by the combination of bearing and bypass stresses.

$$F_{bry} \leq f_{brg} + f_{c_{gross}}$$

The observed failure was by delamination of the splice plates between the innermost bolts, initiated immediately in front of the bolts, where the bearing and bypass loads combined. The strength prediction of 357,000 pounds for this 6-inch-wide and 1-inch-thick skin laminate had been made on the basis of a allowable combination of 100 ksi for  $F_{brg}$  and the critical location had been anticipated to be in the skin at the outermost rows of fasteners. Because of the better clamp-up there, the joint was reanalyzed with an increased allowable of 120 ksi. As a result of the bolt bending shown in Figure 15, the corresponding allowable for the splice plates was reduced to 80 ksi to reflect some loss of benefit from the clamp-up. The analysis then agreed with the test, in regard to both the failing load and the location of failure.

The failure of these specimens, JC12CF and JC12IF, suggests the existence of a new failure mode. The initial delaminations of a pin-loaded hole occur at about 60 ksi in bearing and, in the absence of compressive bypass loads, do not spread catastrophically. However, unless there is adequate clamp-up, as in the middle of a sandwich, those initial delaminations could interact with any compressive bypass stresses and spread catastrophically. Such clamp-up was certainly lacking in these splice plates as the bolts bent under load.

The same phenomenon is believed to have triggered the failure in the compressive tests on the multirow joints with tapered splice plates. These specimens, having four rows of bolts in three columns, were identical to the corresponding tensile specimens described above. Specimens JC24CF and JC24IF failed by massive delaminations of the central region of the splices, as shown in Figure 22. The

specimens were stabilized against overall buckling, so the failure is believed to have been triggered by the combination of high bearing and bypass stresses in compression. The failure of both specimens occurred at gross-section strains of 0.0062 in the skin outside the joint, indicating that the tensile strength limits are more severe, at about 0.0050. These high compressive strains, without failure in the skin, were achieved by the combination of low bearing stresses (about 35 ksi) in the skin and good clamp-up between the splice plates. The failing loads of the splice plates, 297,000 and 302,000 pounds, are between the 277,875 and 321,343 pounds derived by analysis for ultimate combined bearing stresses of 60 and 70 ksi, respectively, in the splice plates. Even the predicted load of 343,930 pounds to fail the joints in compression is not unreasonable, but the location of the anticipated failure as being in the skin was erroneous.

In concluding this section on the subcomponent testing, it should be noted that most of the weaknesses were found to be in the splice plates, which have lower allowables than the skins with better clamp-up, and in excessive bending of many of the bolts. One key to structurally efficient bolted joints in fibrous composites is a low working stress in bearing which permits maximization of the bypass stress and hence the total stresses in the joint. Another is to use stiff bolts having a sufficient diameter to not bend under the applied loads.

## 7. COMPOSITE WING JOINT CONCEPTUAL DESIGN

Beyond the test and analysis activities described above, the program included a preliminary design of a composite wing for a high-technology commercial transport aircraft for the 1990s (Figure 28.) This was done to enough depth to enable conceptual design of major joint areas.

The outer wing was conceived as manufactured in two segments, each approximately 35 feet long. These were bolted to each other and the resulting half-wing joined to the wing center section at a major wing-fuselage intersection joint, as shown in Figure 29. The figure also displays the high spanwise loads in this wing. The wing box geometry was modeled in the Computer-Aided Design and Drafting system. Sections were cut at the two joint areas to obtain loft lines. Skin and stringer thicknesses and stringer spacing were designed and optimized for ultimate loads near the two stations, assuming a 37.5-percent 0-degree, 50-percent  $\pm 45$ -degree laminate with the toughened epoxy, thick-ply graphite fiber material system described above.

The laminate design criteria for the composite wing cover are given below:

- Upper panels carry ultimate compression loads
  - Theoretical skin, local and general buckling calculation
  - No skin buckling at limit load
- Disallow use of concentrated 0-degree,  $\pm 5$ -degree plies  
Maximum directional interspersing of thick plies (0.010 inch/ply)  
Provisional axial/biaxial strain cutoffs:
  - 0.00525 tension ultimate
  - 0.0045 compression ultimate

WEIGHT SUMMARY (LB) MODEL D-3243-22	
MAXIMUM TAKEOFF	213,500
MAXIMUM LANDING	194,000
MAXIMUM ZERO FUEL	180,000
FUEL CAPACITY (AT 6.7 LB/GAL)	85,580
MANUFACTURER'S EMPTY WEIGHT	122,815
OPERATOR'S ITEMS	4,885
OPERATOR'S EMPTY WEIGHT	127,700
MAXIMUM PAYLOAD	52,300

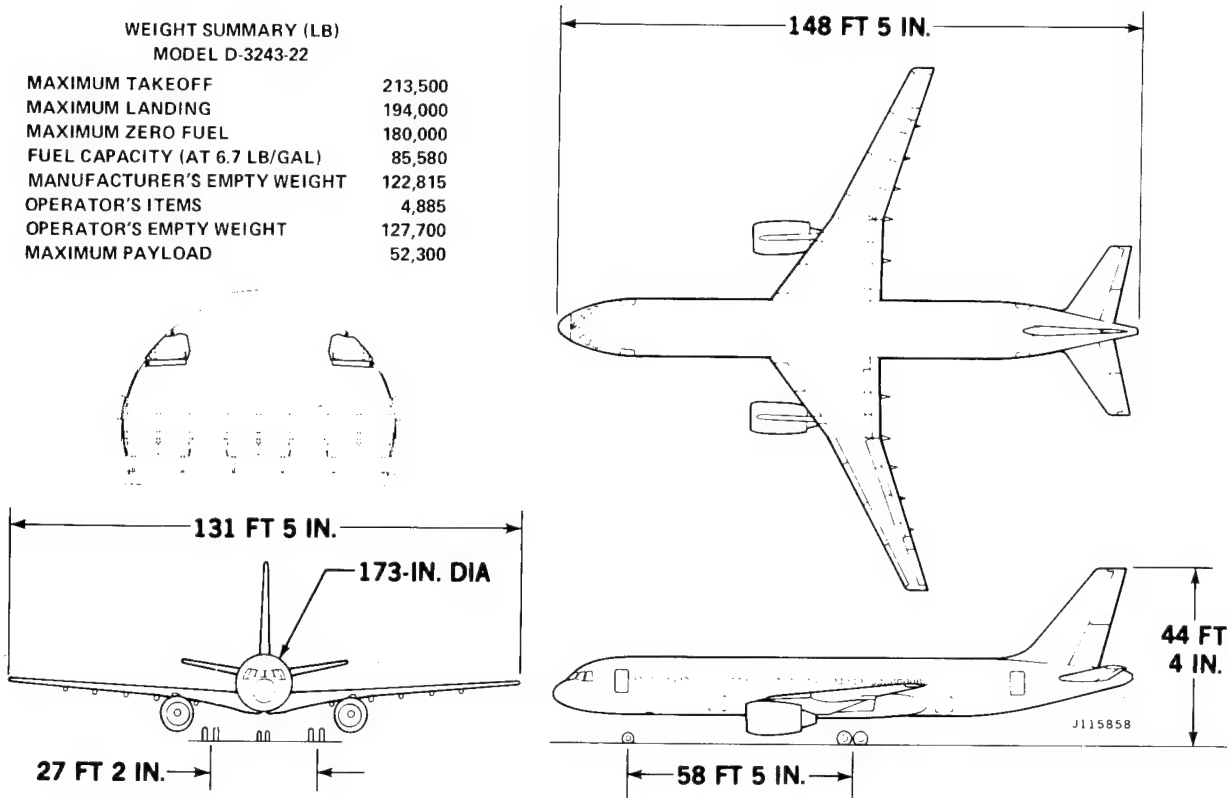


FIGURE 28. BASELINE AIRCRAFT CONFIGURATION

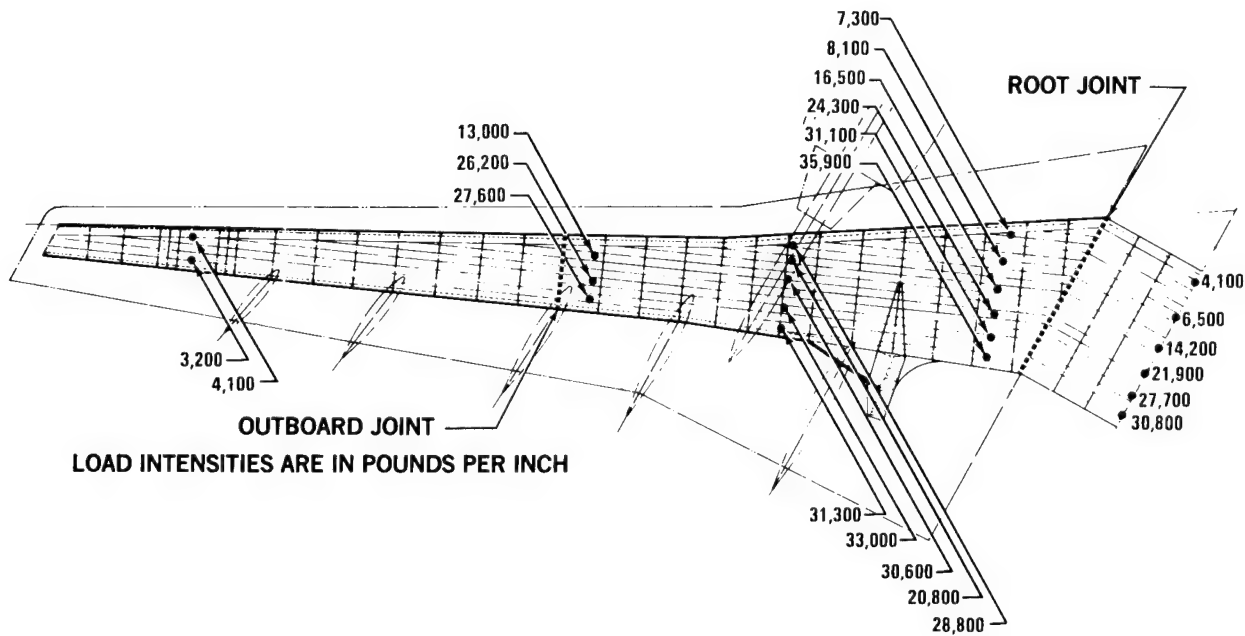


FIGURE 29. WING LOAD INTENSITIES AND JOINT LOCATIONS

- Damage tolerance: inherent in strain cutoff
- Tension fatigue: not considered in preliminary sizing since multirow bearing stresses are generally low
- Meet minimum torsional (GJ) and wing-bending (EI) stiffness requirements of metal wing.

They include an ultimate load allowable strain anticipated to be compatible with a requirement to carry moderate damage at limit load in a toughened epoxy material system. It should be noted that these criteria are considerably more optimistic than the 0.002 to 0.003 strain criteria previously used in production for damage-tolerant composite primary structure. Although this program was not designed to establish wing laminate design strain levels or damage-tolerant designs, target criteria were necessary to establish preliminary joint designs.

Design strains for laminate patterns of interest to wing skin design were chosen above 0.003 to allow weight savings as compared to aluminum structure, which is normally designed in the 0.0045 to 0.006 range.

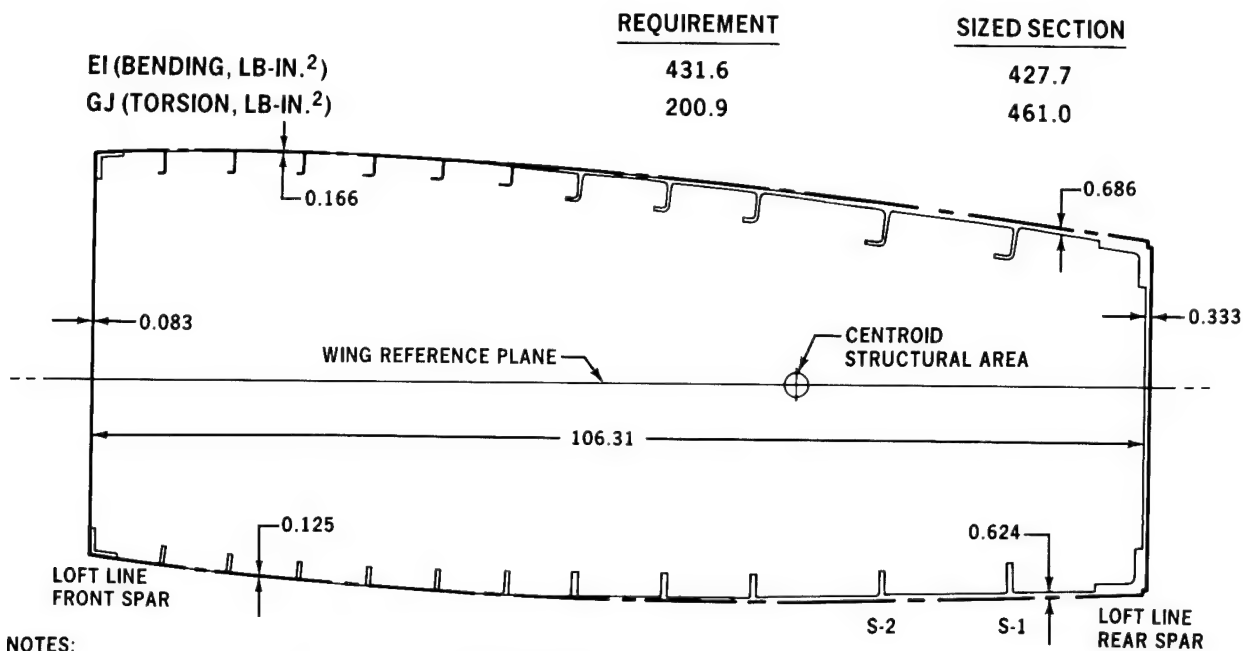
Although skin buckling is allowed above 0.003 strain with stringer plus effective skin-carrying ultimate load, this occurs only in more lightly loaded areas where the laminates are thin enough to buckle without cracking. General rather than local stability governs the design sizing of much of the wing cover for this highly loaded wing.

Integral blade stringers stiffen the lower (tension) cover and integral J-stiffeners are used for the upper (compression) cover. Near the wing root, due to a running load approaching 36,000 pounds per inch concentrating near the rear spar, a wide 13-inch stringer spacing is appropriate for the thickest skins, with closer spacing used in areas toward the front spar where loading is less and the skins are thinner (see Figure 30.) This design causes less interruption to the skin splices in the most highly loaded areas and minimizes the problem of stringer runouts in the same areas. The section shown in Figure 30 meets the metal wing bending (EI) and torsional (GJ) stiffness requirements; however it was necessary to increase the strength-designed percentage of spanwise 0-degree fibers to 42 percent in order to meet the bending stiffness required without weight penalty. The same design procedure was followed at the outboard joint section, and it was again necessary to utilize a 42-percent 0-degree laminate to meet section bending stiffness requirements. In both cases, excess torsional stiffness existed in the sized composite sections due to a higher percentage of required material being in the skins with respect to the usual skin/stiffener ratio of metal wings.

Since the wing preliminary design activity was scoped to obtain only sized and realistic transitions to joint areas, it was not appropriate to optimize the flutter analysis in order to accommodate the strength-designed laminate properties. In retrospect, it is apparent that designing composite wings to metal wing EI and GJ distributions can introduce a weight penalty if the decoupled E and G weight reduction potential of composite laminate is not accommodated by flutter analyses which redistributes EI/GJ to optimize for the composite.

## DEVELOPMENT OF CONCEPTUAL JOINT DESIGNS AND CRITERIA

At the beginning of the program, current joint theory stated that at single loaded holes (single-row bolted joints) in pseudoisotropic Narmco 5208/T300 material, 0.0055 inch/ply, the maximum allowed joint gross-section strain away from the holes would not exceed about 0.0035 at an optimum w/d of about 3.0. Laminates of greater percentage 0-degree fibers would achieve lower joint strains [1].



NOTES:

- INITIAL SIZING WITH (37.5/50/12.5)% , 0/±45/90-DEGREE LAMINATE
- EI REQUIREMENT MET WITH (42.5/45/12.5)% LAMINATE
- GJ EXCESS DUE TO STIFFENING RATIO LESS THAN METAL WING AND THICK PLY RESTRICTIONS ON MINIMUM GAUGE
- SPAR WEBS ARE PSEUDOISOTROPIC PATTERN

FIGURE 30. COMPOSITE WING ROOT RIB SECTION AND STIFFNESS PROPERTIES

However, a small increase in percentage of 0-degree plies is associated with a higher modulus and a small increase in overall strength because the laminate strength increases slightly faster than the associated stress concentration factor at the bolt holes. Specifically, Pattern B is on the order of 10 to 15 percent better than Pattern A for high-aspect-ratio wings. Multirow joints with splice plate tapering were shown in the present program to offer higher joint strain capability due to reduction of bearing stress at the critical hole row. Multirow joints were, of course, necessary to carry the high wing joint loads with reasonable fastener sizes.

The preliminary joint design criteria selected for the basic 37.5-percent 0-degree laminate (Pattern B) restricted joint strains to a range between 0.0032 and 0.004, depending on bolt sizes. This was based on experimental runs of A4EJ to determine the optimum w/d for multirow generic joints of the type designed for the subcomponent test series. Later analyses, using ancillary test data to construct A4EJ bearing/bypass inputs, demonstrated that the 0.004 to 0.005 strain range was achievable with careful joint tailoring and greater bypass load-carrying ability of the Ciba Geigy 914 10-mil material. These design analyses indicated multirow joints optimized at a w/d greater than 3; i.e., in the range of 4 to 5. Thus, sufficient confidence was gained to initiate multirow conceptual joint designs with generous w/d column spacing to maximize the bypass load. As described earlier, advantage was taken to further optimize the joints with smaller fasteners in the first row and larger fasteners in the last, or inside, row.

Titanium bolts in close-fit holes were selected for material compatibility and were allowed to work at a rated shear strength efficiency no greater than 0.75. Bolt sizes with shear efficiencies much lower than that are, in fact, often required to prevent "bearing yield" effects due to significant bolt bending before the ultimate design load is reached.

Excessive bolt bending was experienced with some subcomponent test specimens having titanium core bolts in interference-fit sleeves. Steel core bolts are recommended for interference-fit sleeved bolt installations used in future designs. The 303 stainless sleeve isolates the bolt from contact with graphite.

Since joint failure strain levels were predicted in the early analysis at less than the laminate ultimate design strains (0.0032 to 0.004 versus 0.0045 to 0.00525), some method was required to reduce strains in the joint. The 42-percent 0-degree skin laminate, based on the wing bending stiffness requirement, is undesirable in joint areas since splitting failure characteristics and higher hole stress concentration factors have been associated with laminates containing greater than 40-percent 0-degree plies [8]. An increase in thickness, or a change of pattern entering the joint, or both may be considered for use to reduce strains, stress concentration factors, and bearing stresses at the bolt holes.

The equation,

$$t_{\text{skin}} (\varepsilon_{\text{sk}} E_{\text{sk}}) = N_x = t_{\text{jt}} (\varepsilon_{\text{jt}} E_{\text{jt}})$$

indicates that the joint reinforcement factor ( $t_{\text{jt}}/t_{\text{sk}}$ ) is the ratio of the skin design strain and stiffness to the joint strain and stiffness at the same load per unit width of joint ( $N_x$ ).

It would be highly desirable to avoid skin reinforcement at joints from the standpoint of both cost and basic skin repairability. The philosophy of pad-ups in the joint areas implies that the basic design areas are too highly strained to permit bolted joints or bolted repairs there; nevertheless, the reinforcement concept exists until it is demonstrated that higher joint strains are achieved by use of multibolt patterns and toughened resin composites. Fortunately, the test and analysis portions of this program demonstrated that 0.005 strain levels are feasible in the 37.5 percent 0-degree joint laminate using a toughened resin materials system, after careful attention is given to bolt load distributions.

In the preliminary wing design, the skin laminate stiffness change to higher percent 0-degree plies without an increase in thickness implied a lowered design strain at design loads. If stress concentration factors are ignored, this strain reduction could be construed as sufficient to avoid increases in skin thickness at joints; however, the transition to the softer 37.5-percent laminate is required to reduce  $k_{tc}$  factors. The pattern change is best accomplished by adding  $\pm 45$ -degree and 90-degree plies rather than stopping 0-degree plies to substitute 90-degree and 45-degree plies. The final joint design strains are thus lowered below 0.005 (tension) in the thickness increase at the joint.

The preceding discussion illustrates that joint reinforcement could not possibly be eliminated for early conceptual design. An example of reinforcement is shown for the lower rear spar at the side of a fuselage splice (Figure 31). The conceptual splice design is shown in Figure 32.

An upper rear spar side of the fuselage joint was also considered. A section through the cap and skin at the integral bulkhead tee splice member is shown in Figure 33. The various concepts show titanium metal used in fittings, tees, and splice members subject to load direction changes or triaxial stress states involving tension. This use of compatible metal precludes loading the composite across its weak interlaminar direction.

$$k_p = \frac{t_p}{t_0} = \frac{\text{REINFORCED THICKNESS}}{\text{BASIC THICKNESS}}$$

$$t_p(E_p\epsilon_p) = t_0(E_0\epsilon_0)$$

SECTIONS LOOKING INBOARD - LEFT WING

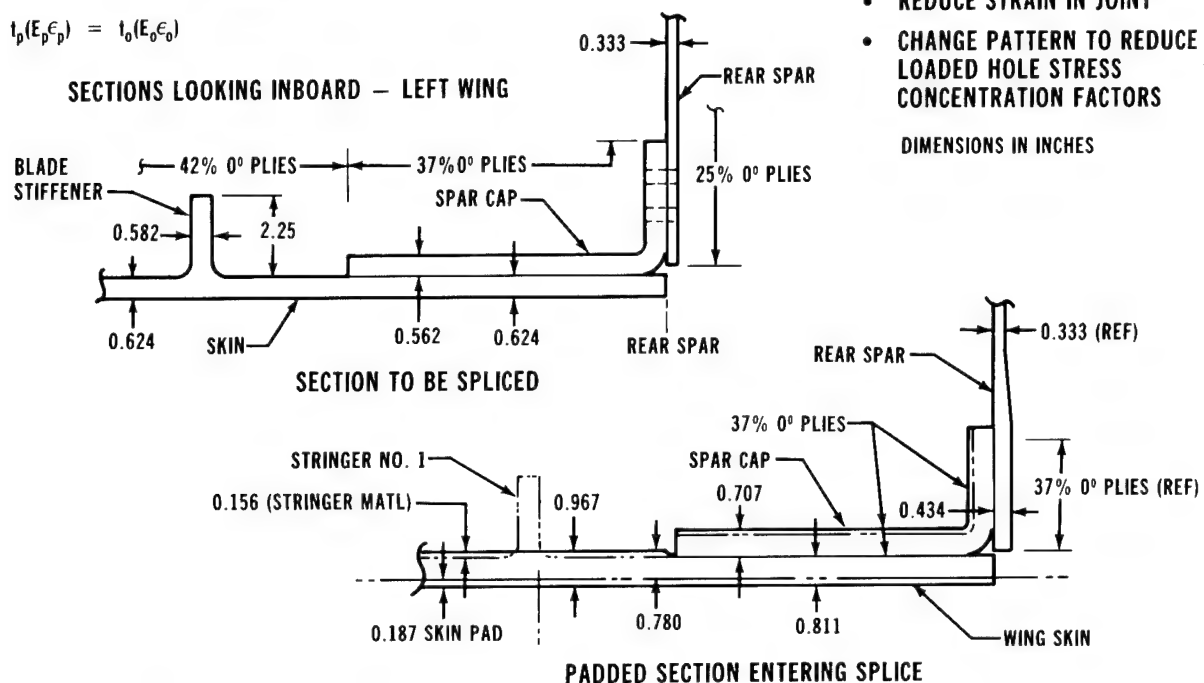


FIGURE 31. BASIC AND REINFORCED SECTIONS AT LOWER REAR SPAR JOINT

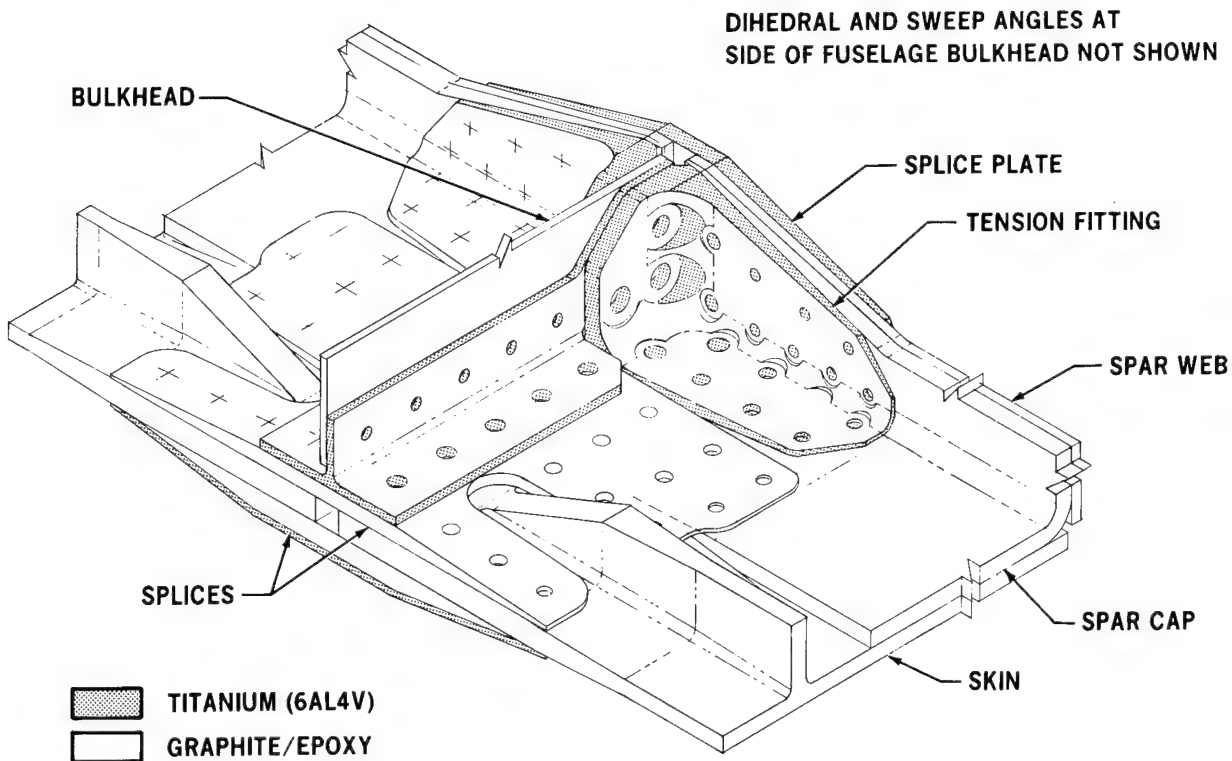


FIGURE 32. LOWER REAR SPAR AND STRINGER CONCEPTUAL JOINT

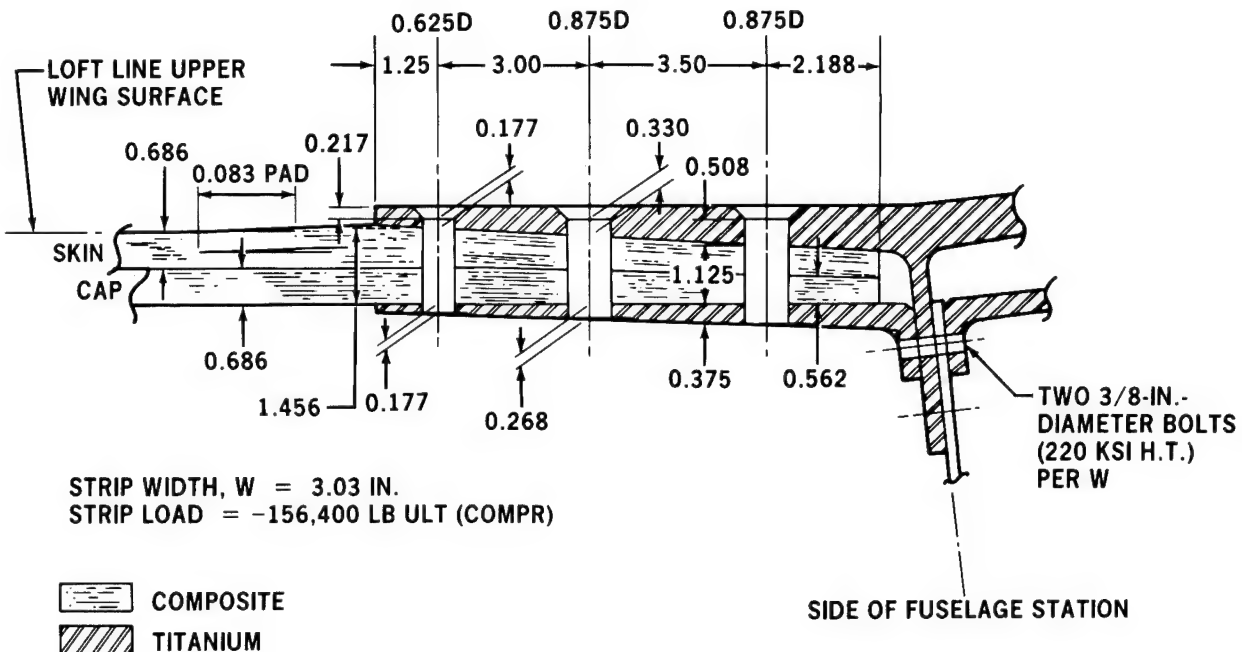


FIGURE 33. UPPER REAR SPAR CAP AND SKIN SPLICE CONCEPT

An outboard upper wing skin and stiffener joint concept is shown in Figure 34. The bulkhead support is not a fuel bulkhead where bathtub fittings would be used rather than the simple plate splices shown.

Design of these joints begins with an educated assumption regarding bolt load distribution and allowed bearing stresses at each hole. The subsequent detailed analysis for bolt load and bearing-bypass interactions would be iterated with design changes to arrive at a final design.

The design issues exposed by the conceptual joint design exercise and the preliminary design criteria utilized in sizing the above joints are summarized below.

#### PRELIMINARY PROCEDURE FOR CONCEPTUAL JOINT DESIGN

The preliminary procedure for conceptual design of a joint is given below:

- The joint laminate allowed strains should not exceed 0.005 and may be as low as 0.003 in the 37.5-percent 0-degree laminate.
- An average bolt size ( $d_{av}$ ) for the load ( $P_w$ ) in a strip ( $w$  wide) should be established, depending on whether single- or double-shear splicing is used. The number of bolts to satisfy the relation  $P_{av} = P_w/kn$  should be used where  $n$  is number of bolts/strip and  $k$  is the bolt efficiency factor not to exceed 0.75.  $P_{av}$  does not exceed the bolt rated single- or double-shear strength, and  $k$  may be less than 0.75 when bolt flexibility effects are taken into account.
- The resulting  $w/d_{av}$  should be compared with other results to see if it is in a range suitable for the bearing and bypass interactions. Usually,  $3.5 < w/d_{av} < 5.0$ , depending on number of bolts in the column.

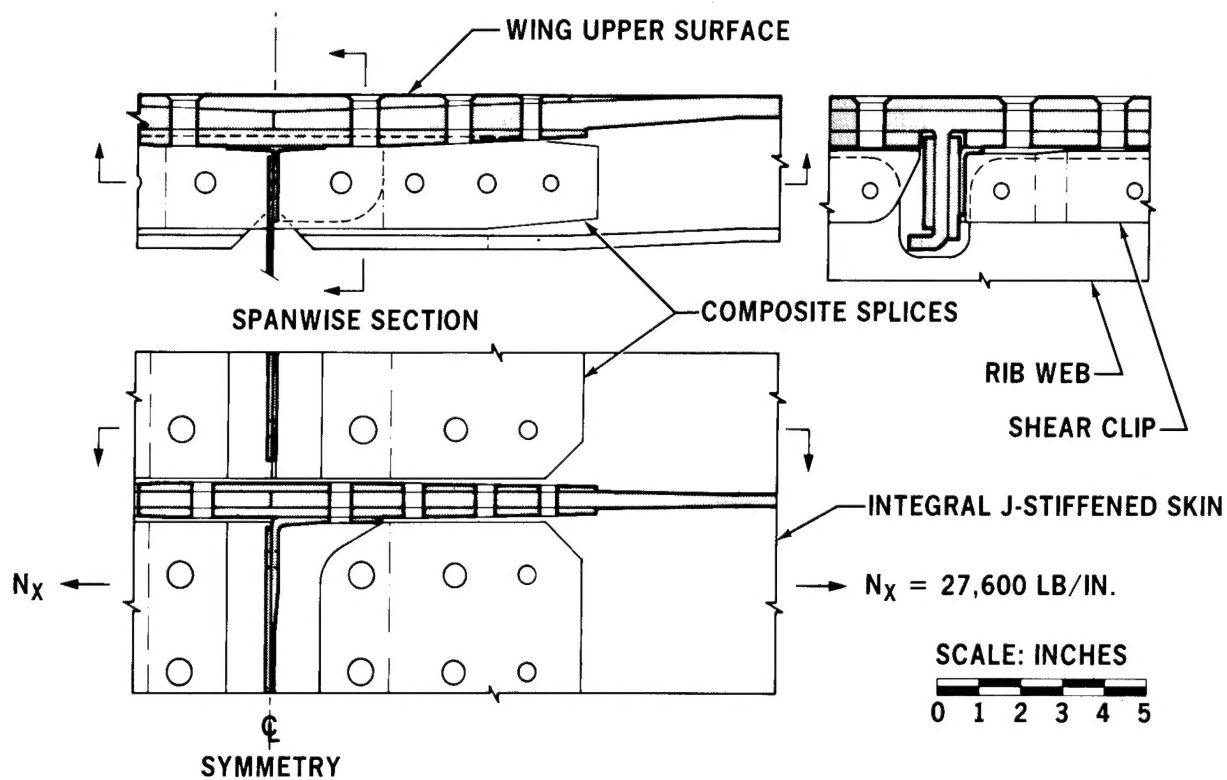


FIGURE 34. OUTBOARD WING UPPER COVER JOINT

- The first bolt entering the joint might be made smaller than the average diameter and the last bolt larger than the average diameter in the base laminate. This would maximize the bypass load at the first bolt, attracting higher loads to the other bolts.
- The splice plate taper and bearing thicknesses should be established to accommodate the bolt load distributions. This assumes a constant-thickness base laminate in the joint. If the base laminate also tapers in thickness, the bearing stresses at the last bolt may limit joint strength.
- Maximum laminate bearing stresses for fatigue are not considered here. However, bearing stresses vary from 30 to 100 percent of the allowable  $F_{BRU}$  in a tailored multirow joint if fatigue is not considered; hence, the designer should consider that the critical bolt may be fatigue-critical depending on bolt fit tolerances.
- The recommended side edge distances are 2.5d and the end distances are 3d minimum to prevent shear-out.

## CONCLUSIONS

The prime conclusion to be drawn from this investigation is that it is possible to make reliable strength predictions for large multirow bolted joints in fibrous composite laminates. Not all geometries or load conditions have been covered yet, and the testing during this investigation has revealed new failure modes, particularly for compressive loading. With efficient joint design, gross-section strains in the basic skin laminates can reach 0.005, which represents a considerable improvement over the prior state of the art, even for only room-temperature tests.

The most efficient joints have uniform unreinforced skins to maximize the quality of the laminates and to permit straightforward and bolted repairs in service, in combination with reinforced tapered splice plates. Other joint geometries have been shown to be less efficient, both by analysis and test.

The key to obtaining high operating strains in bolted joints in fibrous composite laminates is in restricting the bolt bearing stresses in the most critically loaded locations. The ability to do this depends on the availability of a good load-sharing analysis, such as the A4EJ program, and sufficient test data to provide the input. Nevertheless, many close predictions have been made based on educated guesses where insufficient data were available. The nonlinear capability of the program, permitting some bolts to fail in bearing but still carry loads while others accept more, is believed to be necessary for accurate ultimate strength predictions.

The failure of most efficiently designed multirow bolted joints is governed by bearing-bypass load interactions in tension and compression and cannot be explained adequately on the basis of separate bearing and net-section allowables. There is also a strong influence from the presence or absence of through-the-thickness clamp-up for both tensile and compressive loads.

The joint strengths attainable are sensitive to the joint geometry as well as to the fiber and resin employed, although they are insensitive to other minor changes in fiber pattern throughout the optimum design region, which includes the quasi-isotropic layup. For HTS graphite-epoxy laminates, the optimum w/d ratio is on the order of 3 for single-row joints and is more likely to be in the range of 4 to 5 for multirow joints. In all cases, there must be adequate edge distance (a minimum of 3d) to prevent shear-out failures.

The strength of bolted joints in composite laminates is limited by the brittleness of the 350°F cured epoxy resins. It is therefore vital to intersperse the plies as much as possible and not to stack parallel plies together. This program did not attempt to resolve whether 0.010-inch or 0.005-inch tapes are superior — all that can be said is that the analyses have been confirmed for both thicknesses. The more widespread delaminations associated with the thicker plies appear to be of benefit with tensile loading and to be a tolerable weakness for compressive loading. However, other fiber-resin combinations could exhibit quite different behavior in this regard.

The high gross-section strains exhibited by the bolted joints tested here indicate that highly loaded primary composite structures are feasible, but require more careful design than is customary for ductile metal alloys.

## REFERENCES

1. Hart-Smith, L. J., "Bolted Joints in Graphite-Epoxy Composites." NASA CR-144899, January 1976.
2. Hart-Smith, L. J., "Design Methodology for Bonded-Bolted Composites Joints," USAF Contract Report AFWAL-TR-81-3154, v. 1, February 1982. (Available from DTIC as AD A117 342.)
3. Garbo, S. P. and Ogonowski, J. M., "Effect of Variances and Manufacturing Tolerances on the Design Strength and Life of Mechanically Fastened Composite Joints," USAF Contract Report AFWAL-TR-81-3041, v. 1-3, April 1981. (Available from DTIC as AD A101 657.)

4. Tate, M. B., and Rosenfeld, S. J., "Preliminary Investigation of the Loads Carried by Individual Bolts in Bolted Joints," NACA TN 1051, May 1946.
5. Crews, J. H., Jr., "Bolt-Bearing Fatigue of a Graphite/Epoxy Laminate," Joining of Composite Materials, ASTM STP 749, K. T. Kedward, Ed., American Society for Testing and Materials, 1981, pp. 131-144.
6. McCombs, W. F., McQueen, J. C., and Perry, J. L., "Analytical Design Methods for Aircarft Structural Joints," AFFDL-TR-67-184, January 1968. (Available from DTIC as AD 831 711.)
7. Hart-Smith, L. J., "Mechanically-Fastened Joints for Advanced Composites - Phenomenological Considerations and Simple Analyses." Fibrous Composites in Structural Design, Edward M. Leno, Donald W. Oplinger, and John G. Burke, eds., Plenum Press, c.1980, pp. 534-574.
8. Garbo, S. P., "Effects of Bearing/Bypass Load Interaction on Laminate Strength," USAF Contract Report AFWAL-TR-81-3144, September 1981. (Available from DTIC as AD A108 006.)
9. Bunin, B. L., "Critical Composite Joint Subcomponent - Analysis and Test Results," NASA CR-3711, 1983.

1. Report No. NASA CR-3710	2. Government Accession No.	3. Recipient's Catalog No.	
4. Title and Subtitle  CRITICAL JOINTS IN LARGE COMPOSITE AIRCRAFT STRUCTURE		5. Report Date August 1983	6. Performing Organization Code
7. Author(s) Willard D. Nelson, Bruce L. Bunin, and Leonard John Hart-Smith		8. Performing Organization Report No. DP 7266	10. Work Unit No.
9. Performing Organization Name and Address Douglas Aircraft Company McDonnell Douglas Corporation 3855 Lakewood Boulevard Long Beach, California 90846		11. Contract or Grant No. NASI-16857	13. Type of Report and Period Covered Contractor Report Nov. 81-Jan. 83
12. Sponsoring Agency Name and Address National Aeronautics and Space Administration Washington, DC 20546		14. Sponsoring Agency Code	
15. Supplementary Notes Presented to Sixth Conference on Fiberous Composites in Structural Design New Orleans, Louisiana, January 24-27, 1983 Langley Technical Monitor: Andrew J. Chapman			
16. Abstract A program was conducted at Douglas Aircraft Company to develop the technology for critical structural joints of composite wing structure that meets design requirements for a 1990 commercial transport aircraft. The prime objective of the program was to demonstrate the ability to reliably predict the strength of large bolted composite joints. Ancillary testing of 180 specimens generated data on strength and load-deflection characteristics which provided input to the joint analysis. Load-sharing between fasteners in multirow bolted joints was computed by the nonlinear analysis program A4EJ. This program was used to predict strengths of 20 additional large subcomponents representing strips from a wing root chordwise splice. In most cases, the predictions were accurate to within a few percent of the test results. In some cases, the observed mode of failure was different than anticipated. The highlight of the subcomponent testing was the consistent ability to achieve gross-section failure strains close to 0.005. That represents a considerable improvement over the state of the art.			
17. Key Words (Suggested by Author(s)) Advanced Composite Structures Structural Joints Structural Analysis Weight Reduction		18. Distribution Statement REDD Distribution Subject Category 24	
19. Security Classif. (of this report) Unclassified	20. Security Classif. (of this page) Unclassified	21. No. of Pages 42	22. Price

Available: NASA's Industrial Applications Centers

NASA-Langley, 1983